Spring 5-17-2018

Chronic Nerve Interfacing Utilizing Graft-Embedded Regenerative Macro-Sieve Electrodes

Amrita Nishtala
Boston University

WASHINGTON UNIVERSITY IN ST. LOUIS

School of Engineering and Applied Science

Department of Biomedical Engineering

Thesis Examination Committee:
Wilson Ray MD, Chair
Matthew MacEwan PhD, Co-Chair
Dennis Barbour PhD

Chronic Nerve Interfacing Utilizing Graft-Embedded Regenerative Macro-Sieve Electrodes

by

Amrita S. Nishtala

A thesis presented to the School of Engineering
of Washington University in St. Louis in partial fulfillment of the
requirements for the degree of
Master of Science

May 2018

Saint Louis, Missouri

Contents

List of Figures

List of Tables

Acknowledgments

I would like to thank my research advisors, Dr. Wilson Ray and Dr. Matthew MacEwan for their continual support throughout this project. Nathan Birenbaum was an indispensable part of this project with his assistance in testing the Macro-Sieve electrode animals with the TDT system. Nikhil Chandra, Soumyajit Ray, Ying Yan, Manu Stephen, and Youchen Zheng have also been eager to help me out and have been able to feed me with new innovative ideas to constantly ensure that I am learning and always seeking inspiration. A special thank you to my peers Amanda Dicks, Nikhil Juneja, Rishabh Chandak, and Dakota Katz for always helping me out when required and for the constant moral support. I would also like to thank the members of my thesis committee for taking time out of their busy schedules to attend my thesis defense, providing me with constructive feedback, and for their invaluable support throughout the span of the project.

Finally, I would like to thank my parents, Murthy Nishtala, Latha Nishtala and my brother, Arvind Nishtala for the invaluable moral support.

Amrita S. Nishtala

Washington University in St. Louis
May 2018

Dedicated to my parents.

ABSTRACT OF THE THESIS

Chronic Nerve Interfacing Utilizing Graft-Embedded Regenerative Macro-Sieve Electrodes

by

Amrita S. Nishtala

Master of Science in Biomedical Engineering

Washington University in St. Louis, 2018

Research Advisor(s): Wilson Ray, Matthew MacEwan

Custom-designed macro-sieve electrodes represent a novel means of facilitating chronic high specificity nerve stimulation needed to control distal nerve musculature and restore sensorimotor function. Implantation of these electrodes requires the transection of the nerve, which has shown to disrupt muscle fiber distribution. This present study assesses the feasibility of implementing these electrodes in an end-to-side nerve graft. The macro-sieve electrodes were fabricated and micro-surgically implanted into 3.2 cm nerve autografts harvested from the sciatic nerve of 12 male Lewis rats. Electrode-enabled nerve grafts were micro-surgically implanted in an end-to-side manner into donor rat sciatic nerves without the need for a transection of the host nerve. The nerve interface was assessed by selectively stimulating regenerated nerve tissue via implanted sieve electrodes while simultaneously mapping evoked muscle activation and force production at 3 months post-operatively. Micro-surgical implantation of nerve grafts and conduit-based nerve grafts into the sciatic nerve of healthy male rats of 3 months resulted in robust axonal regeneration. The electrode-enabled nerve grafts implanted in the sciatic nerve of healthy male rats showed signs of axonal regeneration through the macro-sieve electrode. Electrophysiological assessment showed preservation of motor function 3 months post-operatively.

Chapter 1

Introduction

Peripheral nerve interface devices represent a novel means of facilitating chronic high-specificity nerve stimulation needed to control distal nerve musculature and restore sensorimotor function following neurological injury. In order to successfully interface the device with the nerve, transection of the target nerve is required during microelectrode implantation. Optimal methods of surgical implantation have yet to be identified. Therefore, it is important to examine the efficacy of a new surgical technique in which regenerative sieve electrodes are integrated into peripheral nerve grafts and applied in an end-to-side neurorraphy to target nerves. With this technique, the clinical methods of application of regenerative electrodes *in vivo* will be advanced and yield new approaches to achieving a stable interface to peripheral nerve tissue.

1.1 Peripheral Nerve Injury and Regeneration

When a nerve is injured, the continuity of the axon is disrupted. The cell body undergoes many profound changes through anterograde (center to periphery) or retrograde (terminal to center) signaling (Bradke, Fawcett, & Spira, 2012). Regeneration typically begins with the formation of growth cones from the nodes of Ranvier. The growth cone undergoes an elongation process upon receiving the signals for it by means of axonal transport (Bradke et al., 2012). While the proximal nerve stumps are preparing for growth, the distal nerve stumps undergo clearance and breakage of fibers through a process known as Wallerian degeneration (Scheib & Höke, 2013). The axons then grow along with the Schwann cells from the proximal nerve stump to the distal nerve stump (Scheib & Höke, 2013).

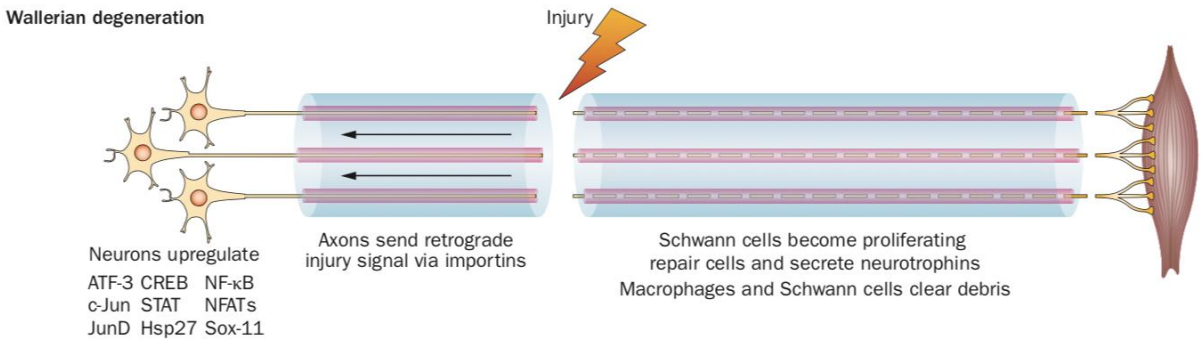

Figure 1.1 Diagram of events that occur after a nerve injury. A retrograde signal is sent to the nucleus where growth-associated genes are upregulated. The distal nerve stump begins degenerating fibers and prepares Schwann cells for regenerating axons to come through.
Source: Jami Scheib and Ahmet Höke. "Advances in Peripheral Nerve Regeneration" *Nature Reviews Neurology* **volume 9**, pages 668–676 (2013). doi:10.1038/nrneurol.2013.227

1.2 End-to-Side Nerve Repair

In the end-to-site "jump graft" model of nerve repair, the distal stump of the injured nerve is co-apted to a side of the donor nerve. Previous studies utilizing this model indicate that functional regeneration occurs across both the proximal and distal portions of the jump graft (Adelson, Bonaroti, Thompson, Tran, & Nystrom, 2004). The two main types of axon growth that occur are regenerative sprouting and collateral sprouting. In regenerative sprouting, axons that are populating in the recipient nerve are derived from sprouts of regenerating units in response to a nerve injury (Pannucci, Myckatyn, Mackinnon, & Hayashi, 2007). In collateral sprouting, the axon that already maintains its contact with the initial target sends sprouts to repopulate the recipient limb and innervate a second target (Pannucci et al., 2007). However further studies have shown that end-to-side repair relies heavily on nerve injury for optimal sprouting (Hayashi et al., 2008). Therefore, this study relies on forming an epineurial window in the recipient nerve to cause regenerative sprouting from the donor nerve. Previous studies have been done on utilizing this model in the sciatic nerve of a rat model (Fujiwara et al., 2007) but the method has yet to be tested for efficacy with neural interfaces such as the conduit and the MSE which are assessed in chapter 3 and 4.

1.3 Nerve Conduits

Peripheral nerve interfaces ensure that regenerating axons at the injury site are not misdirected. Silicone-based nerve conduits are a way to resolve this issue. In the nerve conduit bridging technique, the proximal and distal nerve stumps are inserted into the two ends of the conduit. Axons regenerating from the proximal end to the distal end regenerate and grow into their original pathway in the distal stump (Muheremu & Ao, 2015) (Figure 1.2). Apart from prevention of misdirection, silicone-tubed nerve conduits have been found to produce the essential microenvironment needed for robust nerve regeneration following PNS injuries (Brushart, Gerber, Kessens, Chen, & Royall, 1998). Furthermore, conduits have been proven to assist in better recovery as opposed to direct suturing in animal subjects (Koerber, Seymour, & Mendell, 1989). Nerve conduits of size greater than 1 cm require neutrophic factors for regeneration. However, with conduits as small as 10 mm, as in the case of this study, and nerve regeneration does not require additional growth factors (Pabari, Lloyd-Hughes, Seifalian, & Mosahebi, 2014). In this study, the nerve conduit was incorporated in an end-to-side graft to understand the efficacy of the technique.

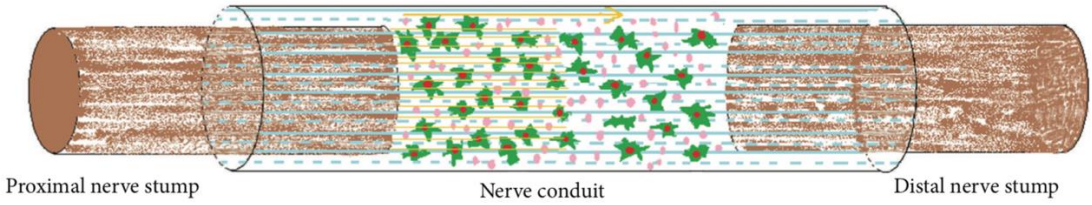

Figure 1.2 Schematic of nerve conduit placement to promote regeneration. (The pink dots represent growth factors that may be added to conduit to further promote regeneration. The green cells represent Schwann cells growing through the conduit)
Source: Aikeremujiang Muheremu and Qiang Ao, "Past, Present, and Future of Nerve Conduits in the Treatment of Peripheral Nerve Injury," BioMed Research International, vol. 2015, Article ID 237507, 6 pages, 2015. doi:10.1155/2015/237507

1.4 Macro-sieve Electrodes

Many of neural prosthetic interfaces serve as an important step in restoring functional movement by bridging the missing connections between severed or damaged nerves (Mensinger et al., 2000). Many instances of extra-neural and intra-neural interfaces have been designed to record and

stimulate peripheral nerve activity. Intra-neural devices are able to make intimate contact with the interfaced nerves, resulting in low excitation thresholds and high recruitment specificity (Branner, Stein, & Normann, 2001; McDonnall, Clark, & Normann, 2004; Yoshida & Horch, 1993). One of the most promising types of neuro-prosthetic interfaces is the regenerative sieve electrode. This electrode is able to innervate within the nerve by allowing nerve regeneration through transit zones (Navarro et al., 2005). Just like the nerve conduit, axons regenerate from the proximal nerve stump to the distal stump. However, in the case of the electrode there is regeneration through the transit zones of the sieve electrode and into the distal nerve stump. The transit zones play a large role in activating all the axons in the nerve, allowing for a more focused and strong regeneration. Smaller transit zones (40 – 65 μm in diameter) cannot activate all the axons in the nerve (Lago, Udina, & Navarro, 2006). In this study, custom designed macro-sieve electrodes with relatively large transit zones (600 μm is the diameter of the electrode) are utilized (MacEwan, Zellmer, Wheeler, Burton, & Moran, 2016). These macro-sieve electrodes (MSE) have a greater transparency factor (MacEwan et al., 2016) and allow for motor neuron fiber regeneration through electrode. Implantation of the MSE requires the transection of the target nerve. Studies have shown that transecting the nerve disrupts the muscle fiber distribution and can lead to muscle atrophy (Higashino et al., 2013; Ijkema-Paassen, Meek, & Gramsbergen, 2001). Therefore, the end-to-side graft has been studied as a possible method of implantation as seen in chapter 4.

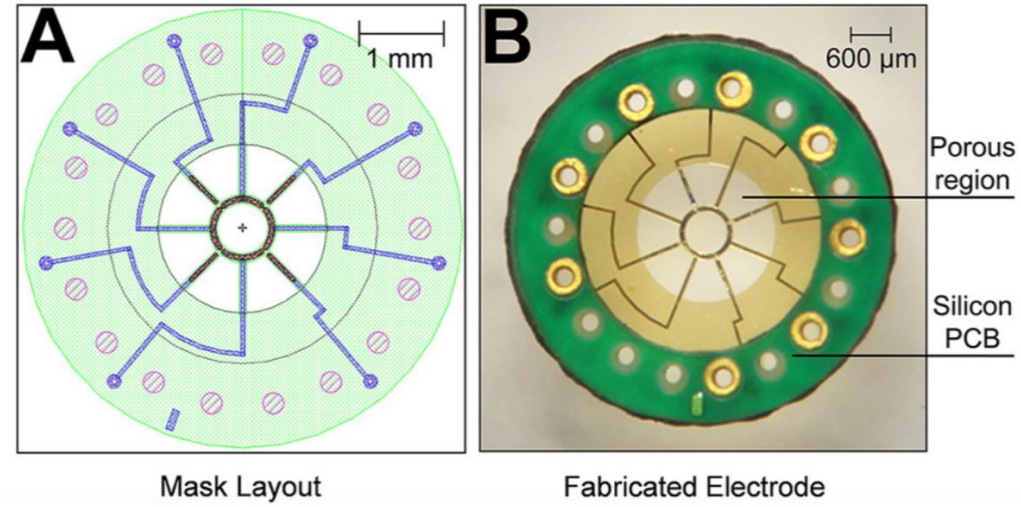

Figure 1.3 Schematic of the Macro-sieve electrode.
Source: MacEwan MR, Zellmer ER, Wheeler JJ, Burton H and Moran DW (2016) Regenerated Sciatic Nerve Axons Stimulated through a Chronically Implanted Macro-Sieve Electrode. *Front. Neurosci.* 10:557. doi: 10.3389/fnins.2016.0055

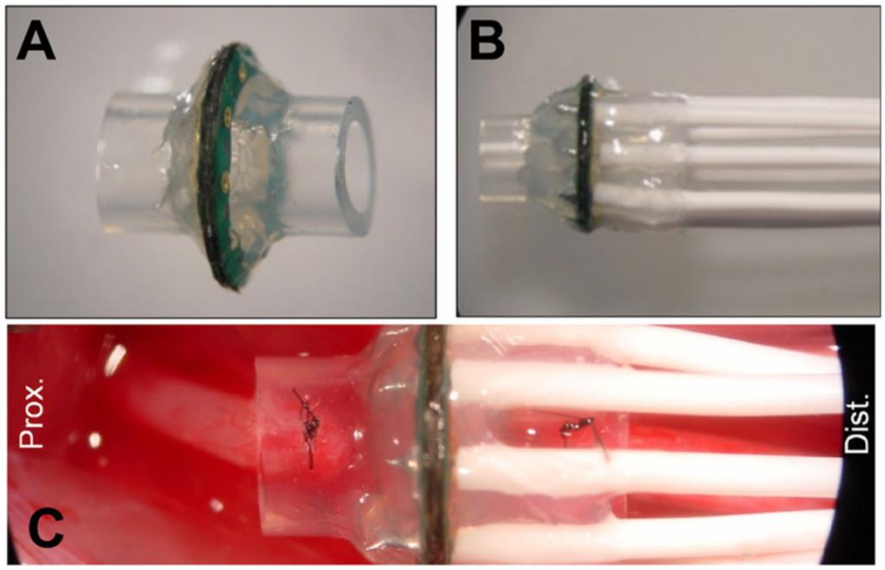

Figure 1.4 Assembly and view of implanted macro-sieve electrode. *Source:* MacEwan MR, Zellmer ER, Wheeler JJ, Burton H and Moran DW (2016) Regenerated Sciatic Nerve Axons Stimulated through a Chronically Implanted Macro-Sieve Electrode. *Front. Neurosci.* 10:557. doi: 10.3389/fnins.2016.00557

1.5 Electrophysiological Assessment

To quantify the regenerative capacity of the axons from the proximal to distal portions, it is necessary to assess the strength of enervation of motor neurons and the muscle fibers. In the studies highlighted the chapters to follow, electromyograms and evoked force measurements are done to quantify this regeneration.

1.5.1 Electromyograms

Electromyograms (EMGs) measure the electrical signal associated with muscle contractions. The functional unit of the muscle contraction is a motor unit, which comprises of the motor neuron and the fiber that it enervates (Raez, Hussain, & Mohd-Yasin, 2006). The muscle fiber contracts when the impulse response, in this case action potentials, hit their depolarization threshold. The depolarization spreads along the muscle, and results in a muscle contraction. Motor units may contain up to 2000 muscle fibers. The motor unit action potential (MUAP) is the summation of all muscle contractions for all the fibers in the motor unit. The EMG amplitude is then a summation of all MUAPs in the given region of electrode placement (Figure 1.5). When stimulus frequency is increased, more action potentials are generated and therefore the EMG values are greater. In nerve injuries, it is important to calculate these EMGs to compare the innervation potential of the regenerated axons to non-injured nerves.

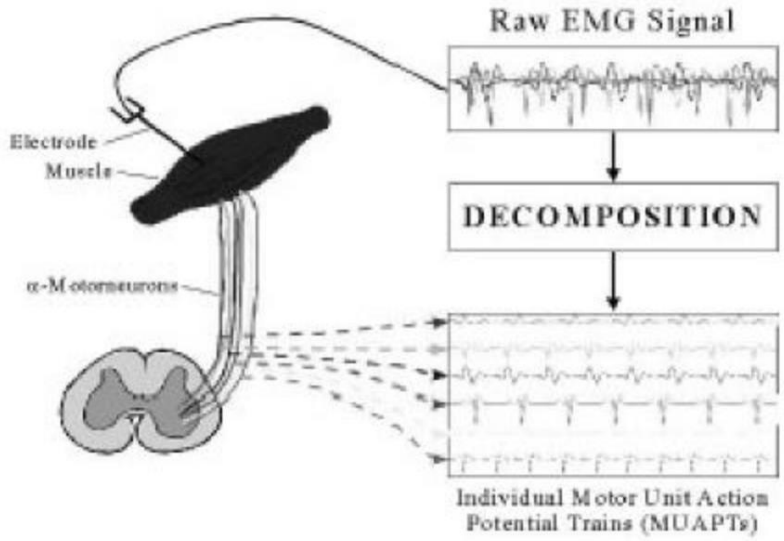

Figure 1.5 Schematic of EMGs
F. *Source:* Raez, M. B. I., Hussain, M. S., & Mohd-Yasin, F. (2006). Techniques of EMG signal analysis: detection, processing, classification and applications. *Biological Procedures Online*, *8*, 11–35. http://doi.org/10.1251/bpo115

1.5.2 Evoked Force Measurement

Upon confirmation of motor neuron and muscle fiber enervation, the strength of the connection can be assessed with evoked force measurements. Twitch contraction measurements are first taken at different stimulus amplitudes to identify the optimal stimulus amplitude that produces the greatest activation force. A twitch is a muscle contraction that occurs in response to a single stimulus that evokes a single action potential in the muscle fiber (Gurfinkel', Levik, & Tsareva, 1984). As stimulus strength increases, more muscle fibers reach their threshold and contract. Thus, the increase in force seen is expected to the increase in the number of contracting muscle fibers (Figure 1.7).

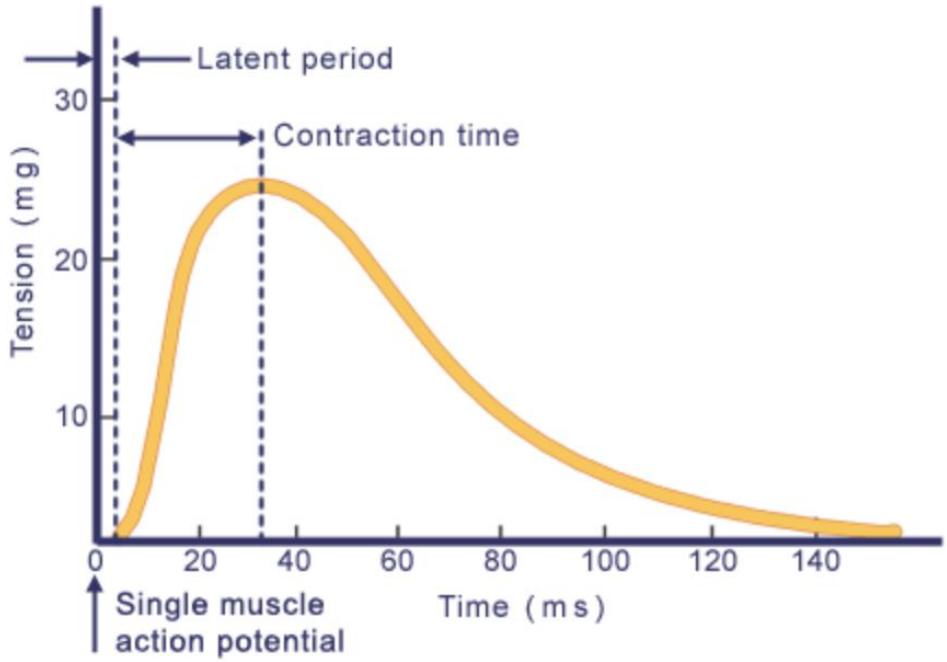

Figure 1.6 Overview of single twitch contraction as seen in skeletal muscle. *Source:* Vander, A.; Sherman, J.; and Luciano D. *Human Physiology: The Mechanisms of Body Function,* 8th ed. New York: McGraw Hill, 2001.

Optimal muscle length is then determined by extending muscle fibers. With longer muscle fibers, the force produced between contractions will be greater.

To determine isometric force production in muscles, the muscle is held at peak stimulus amplitude and peak length. It is stimulated with repeated action potentials are varying frequencies, producing a tetanic muscle contraction (Celichowski, Krutki, Łochyński, Grottel, & Mróczyński, 2004). When stimulated at progressively higher frequencies, there is lesser amount of relaxation of the muscle between twitch, with an increased muscle contraction that occurs until a maximal state of tension is generated (Figure 1.8). After this point, there is muscle fatigue and the repeated twitches will not see as much of an increased muscle contraction.

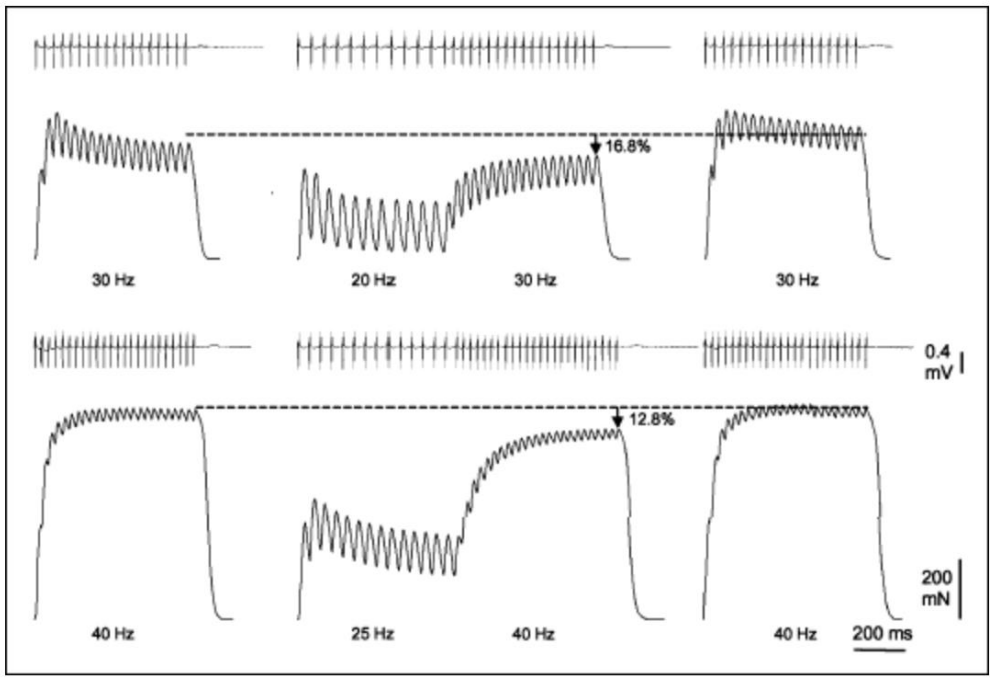

Figure 1.7 Increased stimulus results in increased tetanic force production. *Source:* J. Celichowski, Z. Dobrzyńska, D. Łochyński, P. Krutki Exp Brain Res. 2011 Sep; 214(1): 19–26. Published online 2011 Jul 29. doi: 10.1007/s00221-011-2801-1

1.6 Overview of Experimental Design

The experimental design for this study focuses on evaluating the end-to-side surgical technique in 12 Lewis rats, with 4 animals per group (Table 1.1). The control group is a regular end-to-side repair. The other two groups utilize the nerve conduit and MSE consequently to evaluate the efficacy of this surgical technique.

Table 1.1 Experimental groups utilized in the investigation of jump graft technique. Four animals were utilized in the study per experimental group.

Group	Group I	Group II	Group III
Nerve Conduit	No	Yes	No
MSE	No	No	Yes
	n = 4	n = 4	n = 4

Chapter 2

Group I: End-to-Side Nerve Graft

The end-to-side nerve graft was first tested as a proof of concept with the implementation of the technique without the addition of the peripheral nerve interfaces. Three-months post-surgery, the functional regenerative capabilities of the graft interface were assessed by recording electromyograms (EMG) and evoked muscle force measurements from distal musculature. This chapter highlights the surgery technique and the results of the electrophysiological assessments.

2.1 Experimental Design

Six adult Lewis rats were utilized in this group. A sciatic nerve was harvested from the left and right limbs of two animals to be used as the graft in the other four animals. In the setup of the surgery, the sciatic nerve harvested from the donor animal was sutured to the host sciatic nerve at the sites of a proximal and distal epineurial window. The graft nerve was then sutured in a reverse end-to-side manner where the distal end was sutured to the proximal window (Figure 2.1). A 30-second crush injury just distal to the proximal window was administered to allow for axonal sprouting through the host nerve and into the graft nerve.

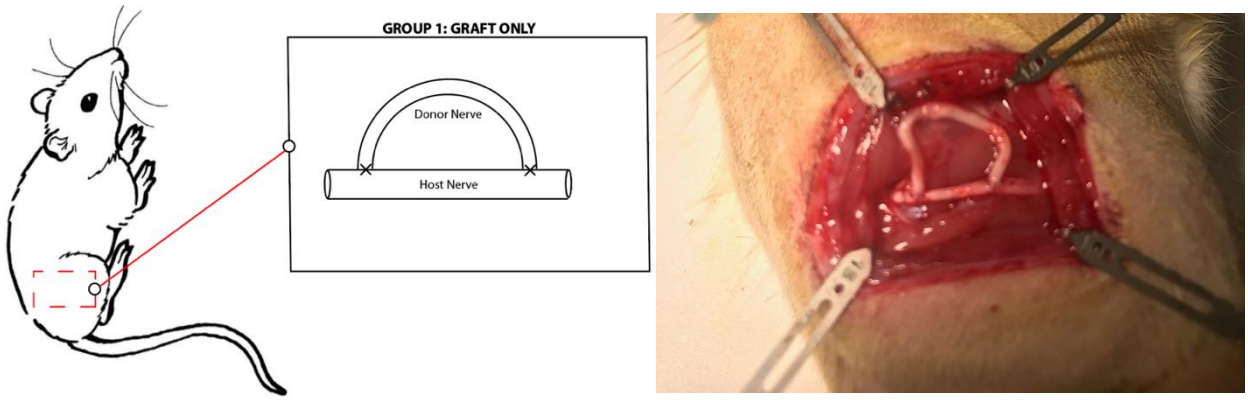

Figure 2.1: Experimental setup. Left panel – a schematic of the surgery. A donor nerve is sutured to the host sciatic nerve at the sites of the epineurial window. Right panel – image of surgery *in vivo*.

2.2 Methods

2.2.1 Surgical Procedure and Setup

All surgical procedures were conducted with aseptic techniques. The Lewis rats were anesthetized by inhalation using 4% Isoflurane/96% oxygen for induction and 2% Isoflurance/98% oxygen for maintenance administered via nose cone inhalation. For maintenance, the 2% Isoflurane was progressively reduced to 1.5% during the course of the surgery in order to reduce the detrimental effects of prolonged inhalation of Isoflurane. The lateral aspects of lower extremities were shaved and sterilized with 70% isopropyl alcohol followed by 7.5% povidone-iodine solution. Following preparation of the incision site, the sciatic nerve was exposed. For this group of animals, micro-scissors were used to create an epineurial window on the proximal and distal ends of the exposed nerve. The 3.2 cm nerve autografts were micro-surgically implanted in an end-to-side manner and sutured at the points of the epineurial windows. At this point, jeweler's forceps were used to administer two subsequent 30-second crush injuries to the native sciatic nerve just distal to the proximal epineurial window to induce axonal sprouting through the window and into the graft.

2.2.2 Electrophysiological Assessment of Nerve Function

2.2.2.1 Electromyogram

The same anesthesia protocol was used for terminal surgery at 3 months to test functionality of nerve regeneration. Trains of monophasic electrical stimuli were applied to the rat sciatic nerve at proximal portions of host and graft nerves while electromyograms (EMGs) were recorded in the *tibialis anterior* (TA) using needle electrodes. Signals were band-pass filtered (LP = 1 Hz, HP = 5 kHz, notch = 6 0Hz) and amplified (gain = 1000X) using a 2-channel microelectrode AC amplifier (Model 1800, A-M Systems Inc., Calsborg, WA) before recording on a desktop computer with a custom data acquisition and software (Red Rock Laboratories, St. Louis, MO). In acquiring data, the epineurial hook electrodes were altered between the graft and host nerves between frequency stimulations. The nerves were also stimulated at the proximal portions. The raw data was then rectified. Average results across trains of stimulation were calculated to yield a measure of evoked EMG responses.

2.2.2.2 Evoked Muscle Force Measurement

The force of evoked motor responses in distal musculature was assessed at 3 months post-surgery to assess force production in re-innervated muscles upon electrical stimulation of the sciatic nerve. Evoked force production was measured in TA and EDL muscles. The distal tendons of the EDL and TA muscles were secured to a thin film load cell (S100) via S-hooks using 5-0 nylon suture. The animals were placed in a custom-designed Functional Assessment Station (FASt System, Red Rock Laboratories, St. Louis, MO) where the right leg was immobilized at the femoral condyles. Twitch contraction measurements were utilized to determine the optimal stimulus amplitude and muscle length for isometric force production in each muscle (Yoshimura, Asato, Cederna, Urbanchek, & Kuzon, 1999). The muscle was first stimulated with incrementally increasing amplitudes at a constant length. The stimulus amplitude at which the largest active force was then recorded. Individual muscle lengths were then increased in 1 mm increments from the relaxed state. The length at which the largest active force was recorded. Tetanic forces were then measured by holding the muscle at peak amplitudes, peak length, and cycling through stimulus frequencies from 0 Hz to 120 Hz. To assess re-innervation of motor axons through the graft and the host into the muscle, the

graft nerve was stimulated at an amplitude first followed by the graft. This cycle was followed through with all steps of measurements. Following all muscle force recordings, the TA and EDL muscles were explanted to obtain wet muscle mass.

2.3 Results

2.3.1 Electromyography Assessment

Electrical stimulation of the sciatic nerve at proximal sites of the graft and host nerves by epineurial silver hook electrodes evoked EMG responses distally in re-innervated musculature (Figure 2.3; Figure 2.4). EMG responses increased with increasing frequencies as seen with the average peak EMG value for each stimulus amplitude (Figure 2.3). Up to 50 Hz the graft and host nerves had similar EMG values. At 80 Hz stimulation, the host nerve and graft nerve, respectively had EMG amplitudes of 8.02 ± 1.20 mV and 6.40 ± 1.75 mV with a difference of 1.62 ± 0.55 mV between the nerves.

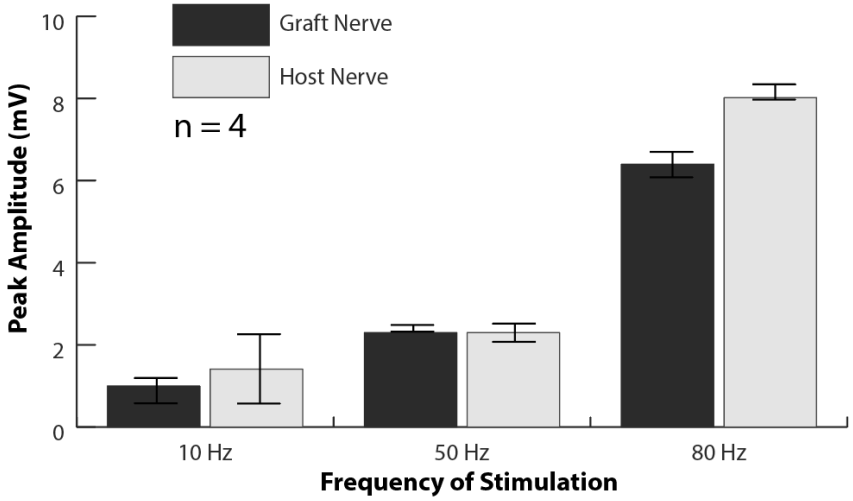

Figure 2.2 Electromyography results. Average peak EMG values for the graft nerve and the host nerve show increase in amplitude with an increase in stimulation frequency. The difference between the peak values for the graft and host nerve at 80Hz is 1.62 ± 0.55 mV.

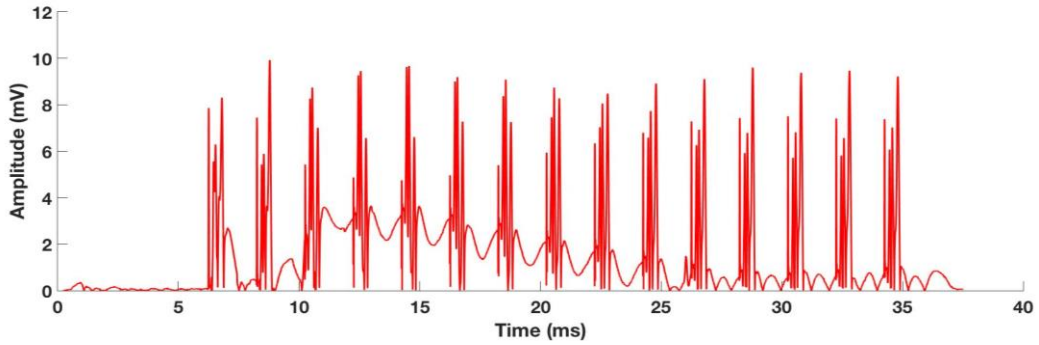

Figure 2.3 Representative electromyograms (EMGs) at 80 Hz recorded distal to the graft nerve. The EMGs were evoked with epineurial hook electrodes at the proximal site of the graft nerve and recorded distally in the TA muscle.

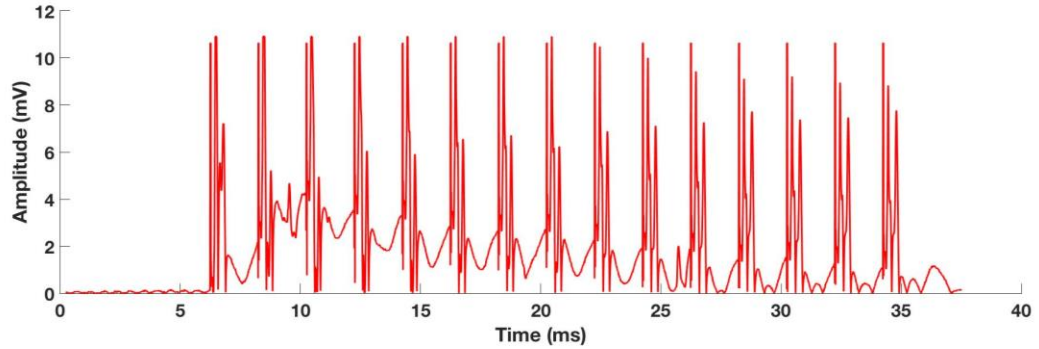

Figure 2.4 Representative electromyograms (EMGs) at 80 Hz recorded distal to the host nerve. The EMGs were evoked with epineurial hook electrodes at the proximal site of the host nerve and recorded distally in the TA muscle.

2.3.2 Evoked Muscle Force Measurement

Stimulus amplitudes increased incrementally while holding muscle length constant. Force production increased as a result of increasing stimulus amplitudes. As expected, stimulation at 1000 μA resulted greatest active force for both TA and EDL muscles (Figure 2.5; Figure 2.7). Stimulus amplitudes beyond 200 μA have been shown to cause nerve damage. Given that this was a terminal assessment, it was interesting to explore the full space and get the full curve. Although the red rock system does not allow for stimulation beyond 1000 μA, force production would be expected to increase till the maximal amplitude was hit. At this maximal amplitude it would be expected that all the muscle fibers

of the TA and EDL muscles would be contracted. The TA and EDL muscle motor axons distal to the graft nerve elicited maximal twitch force measurements comparable to the motor axons distal to the host nerve (TA/Graft: 0.82 ± 1.02 N and EDL/Graft: 0.61 ± 0.76 N, TA/Host: 1.39 ± 0.76 N, EDL/Host: 0.62 ± 1.22 N) (Figure 2.6, Figure 2.8). Specifically, the force production in the EDL was similar for graft and host nerves but was weaker in the graft nerve for the TA. The force production in the graft nerve was generally weaker as compared to the host nerve.

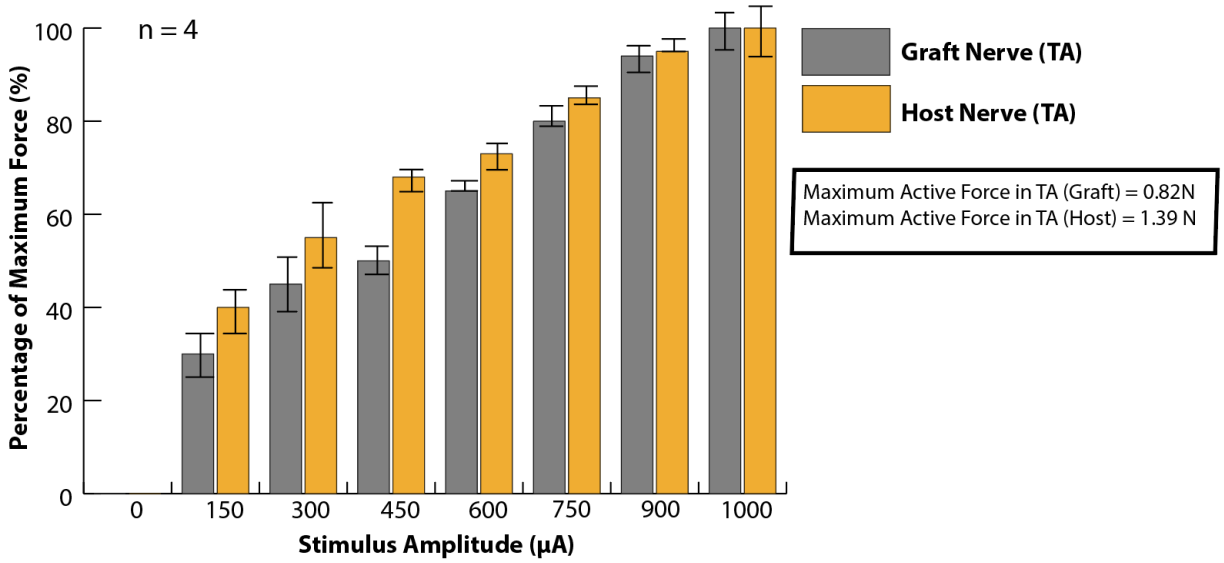

Figure 2.5 Percentage values of twitch force response of TA muscle to stimulation of peripheral nerve tissue. The data for each nerve was independently normalized. Increased twitch contractions with progressively higher stimulation currents are evident.

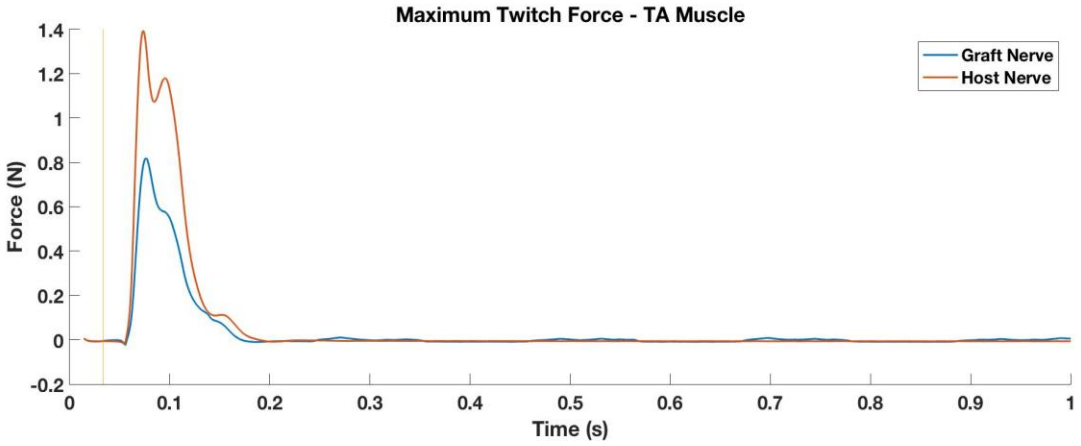

Figure 2.6 TA muscle recruitment curve generated upon stimulation of both nerves at 1000 µA. Elicited maximal force twitch is seen at 0.82 N for the graft and 1.39 N for the host.

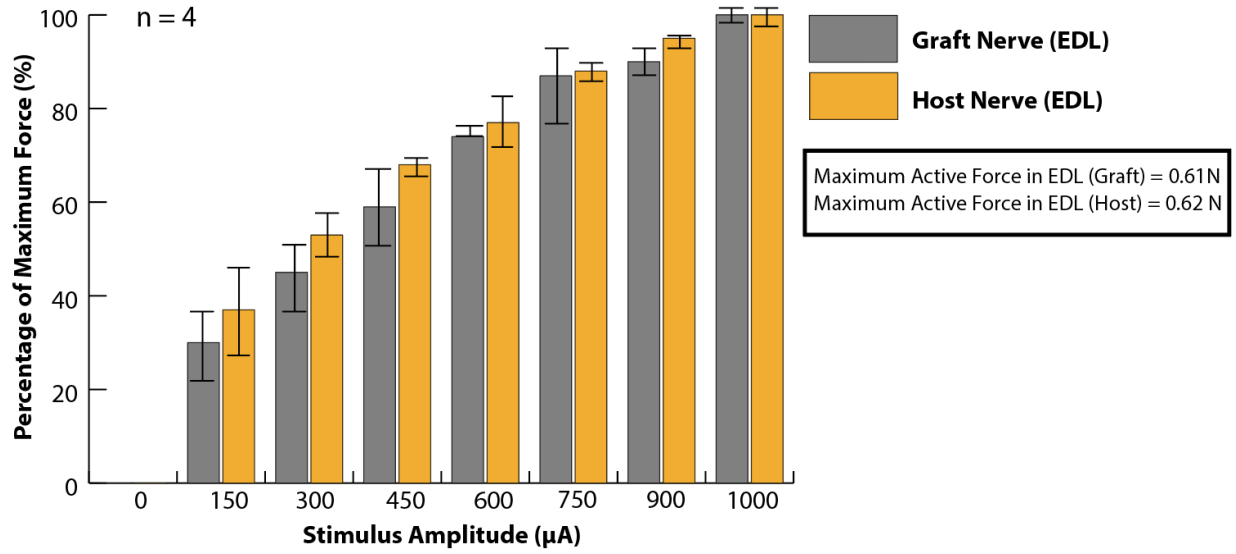

Figure 2.7 Percentage values of twitch force response of EDL muscle to peripheral nerve tissue stimulation. Increased twitch contractions with progressively higher stimulation currents are evident.

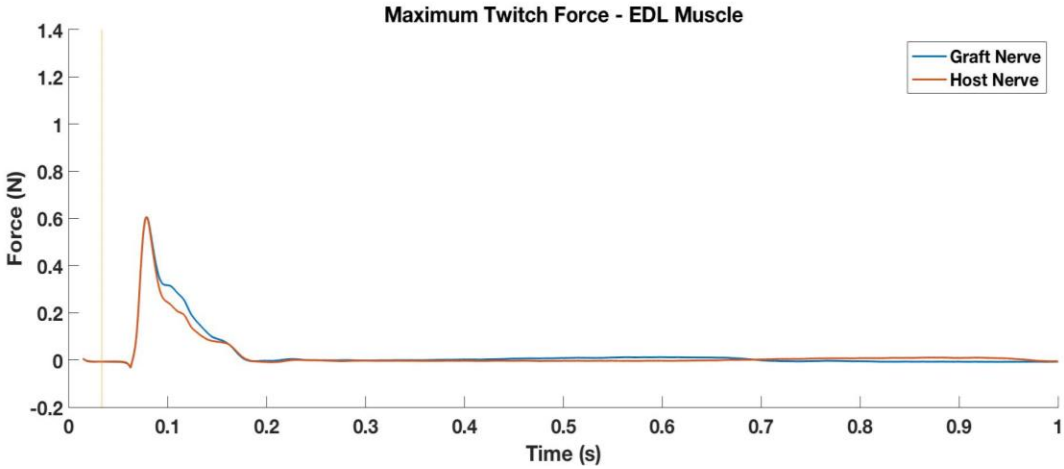

Figure 2.8 EDL muscle recruitment curve generated upon stimulation for both nerves at 1000 µA. Elicited maximal force twitch is seen at 0.61 N for the graft nerve and 0.62 N for the host nerve.

Maximal tetanic force measurements elicited a similar trend (Figure 2.9; Figure 2.11). In both TA and EDL muscles, the largest force was elicited at 80 Hz with a decrease in force thereafter at 100 Hz and 120 Hz. This could have been due to muscle fatigue as a result of repeated stimulation. The TA and EDL muscle motor axons distal to the graft nerve elicited maximal tetanic force

measurements equivalent to the motor axons distal to the host nerve (TA/Graft: 4.35 ± 0.82 N, EDL/Graft: 0.83 ± 0.46 N, TA/Host: 5.25 ± 1.03 N, EDL/Host: 2.37 ± 1.47 N) (Figure 2.10; Figure 2.12). The trends seen in the tetanic measurements followed the twitch measurements, wherein graft nerve stimulation was weaker than host nerve. The TA muscle also generally elicited greater forces as compared to the EDL overall.

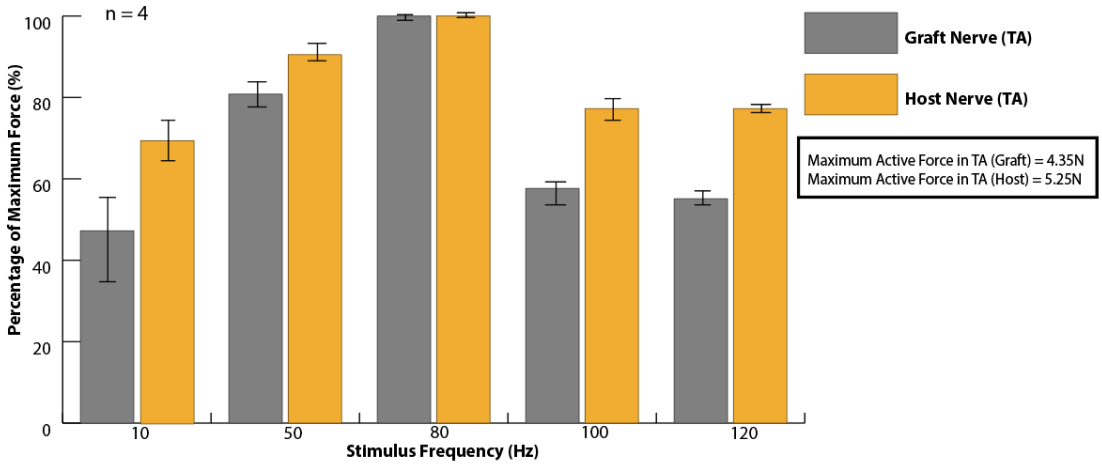

Figure 2.9 A percentage of maximal tetanic force measurements for the TA muscle. Both the graft and host nerves elicited large forces at 80 Hz with a decrease in force at 100 Hz and 120 Hz. This decrease can be attributed to muscle fatigue.

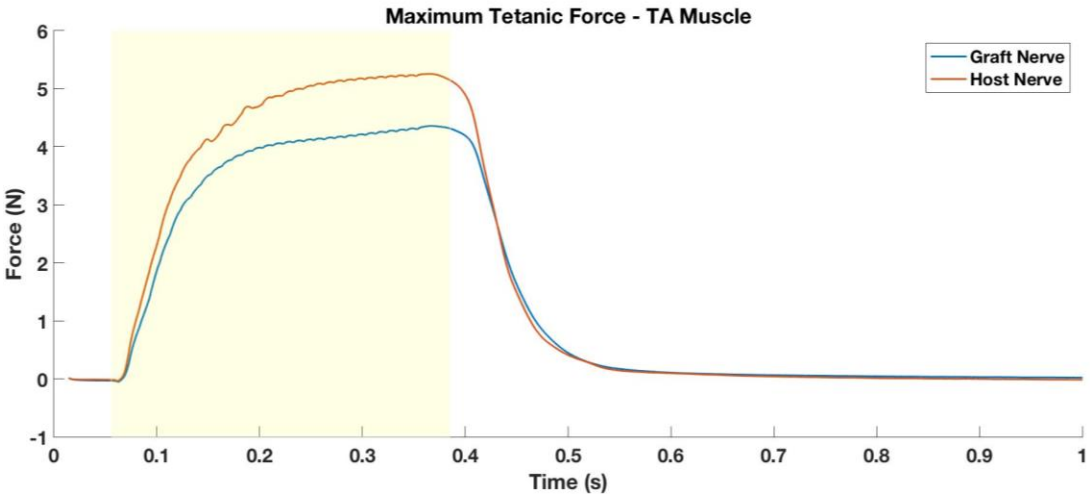

Figure 2.10 TA muscle recruitment at 80 Hz in both nerves. Maximal tetanic force is seen at

4.35 N for the graft and 5.25 N for the host nerve. The rectangular box shows the starting and ending points of stimulation.

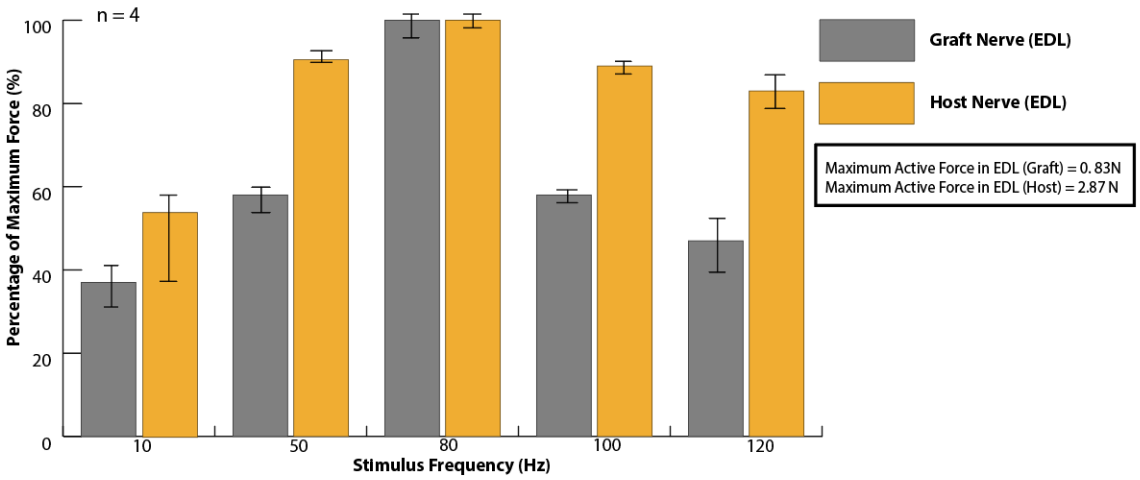

Figure 2.11 A percentage of maximal tetanic force measurements for the EDL muscle. Both the graft and host nerves elicited large forces at 80 Hz with a decrease in force at 100 Hz and 120 Hz. This decrease can be attributed to muscle fatigue.

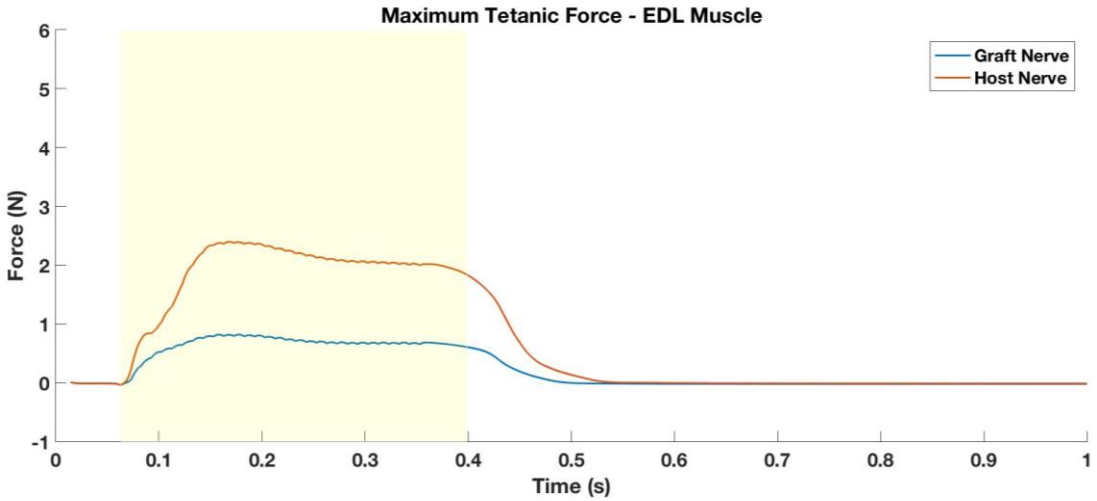

Figure 2.12 EDL muscle recruitment at 80 Hz in both nerves. Maximal tetanic force is seen at 0.83 N for the graft and 2.87 N for the host nerve.

Measurement of wet muscle mass demonstrated similar trends to evoked muscle force measurements. The TA and EDL muscles in the grafted animals also had similar masses when

compared to uninjured or non-grafted animals (Figure 2.13). Therefore, performing this jump graft did not impact muscle mass and did not result in muscle atrophy.

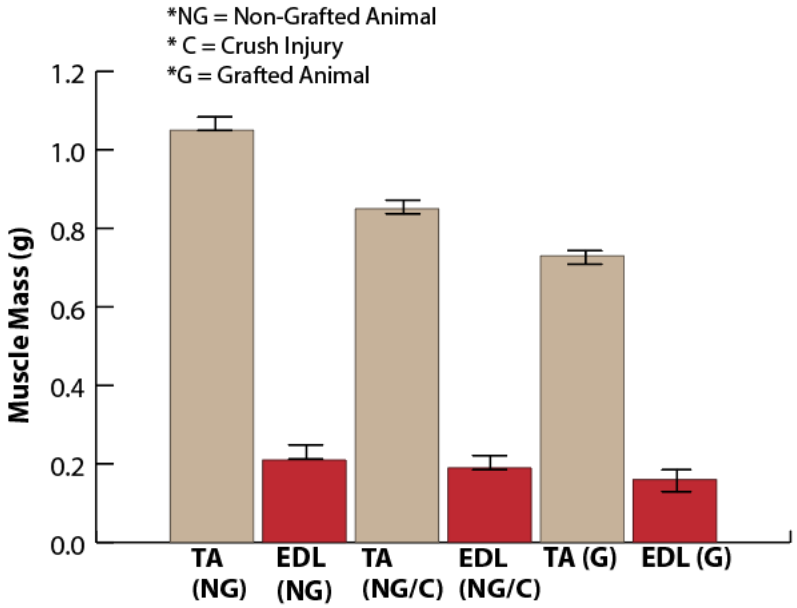

Figure 2.13 Wet muscle mass of TA and EDL muscles following the end-to-side surgery and no injury. The average mass of the TA muscle is slightly lower in the grafted animals while the EDL muscle mass is very similar.

2.4 Conclusions

As a proof of concept, the jump graft or end-to-side method is a feasible technique. The electrophysiological assessments showed indications of motor axons going through the distal portions of the graft and host nerves and re-innervating with the muscle. As expected, the graft nerve had weaker innervation as compared to the host nerve. This is because the motor axons at the distal site of the graft nerve were not previously innervated with the musculature like the host nerve, which resulted in the graft nerve forming new axon networks with muscle fibers.

Chapter 3

Group II: End-to-Side Nerve Graft with Conduit

Currently, the interfacing of the Macro-sieve electrode (MSE) with the nerve can only be done with a transection of the healthy sciatic nerve. Having found that the end-to-side neurorrhaphy results in robust axon regeneration, it is important to understand if the jump-graft technique can be combined with nerve transections. To assess this concept, the jump graft surgical technique was combined with a silicone nerve conduit to allow for site-specific axon regeneration. The host and graft nerves were then assessed for distal motor axon regeneration utilizing the techniques described in chapter 2. Three-months post-surgery, the electrophysiological assessments conducted in chapter 2 were repeated on this group of animals to gather isometric force measurements form distal musculature. This chapter highlights the surgery technique and the results of the electrophysiological assessments.

3.1 Experimental Design

Six adult Lewis rats were utilized in this group. A sciatic nerve was harvested from the left and right limbs of two animals to be used as the graft in the other four animals. In the setup of the surgery, the sciatic nerve harvested from the donor animal was first transected and placed in a silicone conduit. The transected graft nerve was then sutured to the host sciatic nerve at the proximal and distal ends of the exposed nerve (Figure 3.1). The host nerve was injured on the distal to the epinuerial window to allow for regeneration of axons through the distal portion of the graft.

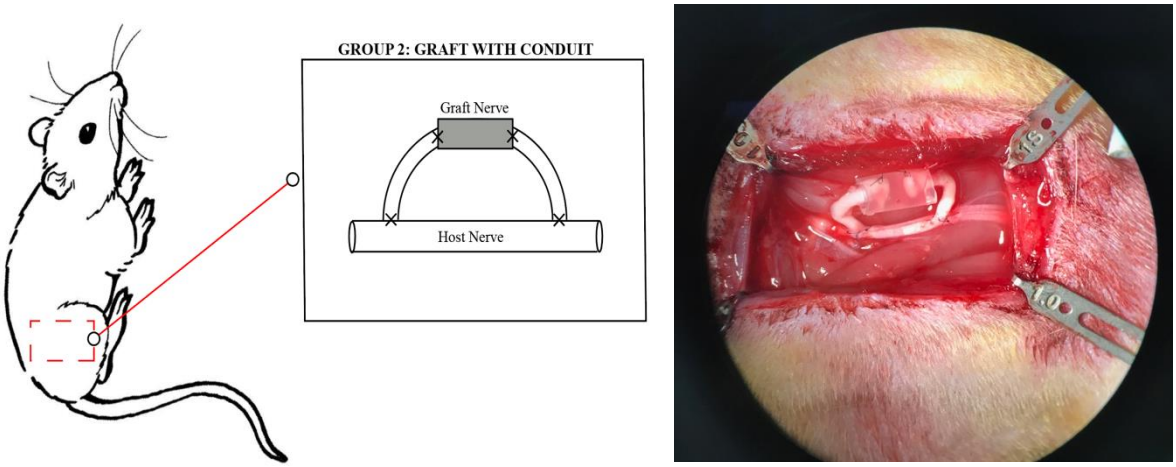

Figure 3.1 Experimental setup. Left panel – a schematic of the surgery. The donor nerve is transected with the proximal side of transection sutured to the left side of the conduit and the distal side sutured to the right side of the conduit. The donor nerve is then sutured to the host sciatic nerve at the sites of the epineurial window. Right panel – image of surgery *in vivo*.

3.2 Methods

3.2.1 Surgical Procedure and Setup

The surgical procedure and setup used in this experiment was similar to the methods described in chapter 2. However, for this group of animals the donor nerve was first transected and sutured to a sterilized silicone conduit prior to the end-to-side surgery.

3.2.2 Functional Assessment

Electromyograms (EMGs) and evoked force measurements followed the same protocol described in chapter 2.

As a recap of stimulation parameters, the stimulus amplitude was held constant at 1000 μA for 0.2 ms while cycling through stimulus frequencies of 10 Hz, 50 Hz and 80 Hz to record EMGs from the TA.

For the evoked force measurements, stimulus amplitudes increased incrementally to find the optimal stimulus amplitude. Peak length was increased incrementally to find the optimal length. Holding these two values, the muscle was stimulated at frequencies 10 Hz, 50 Hz, 80 Hz, 100 Hz, and 120 Hz to obtain tetanic force measurements.

3.3 Results

Three months post-surgery, regeneration through the conduit was evident (Figure 3.2).

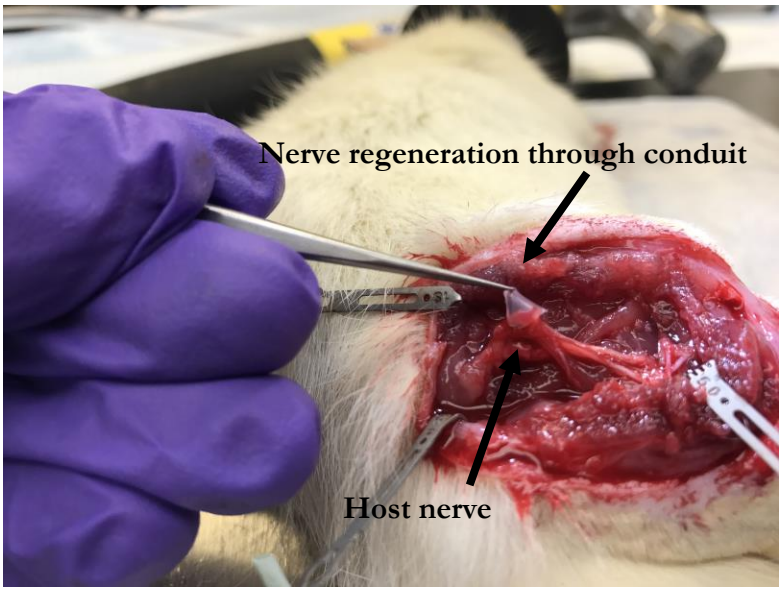

Figure 3.2 Nerve regeneration through the silicone conduit. The nerve regenerated through the conduit has formed the full graft nerve, bridging the gap created at the transection site. The host nerve is also present directly below.

3.3.1 Electromyography

Electrical stimulation of the sciatic nerve at proximal sites of the graft and host nerves evoked EMG responses distally in re-innervated musculature (Figure 3.4; Figure 3.5). The EMG recordings showed effective muscle activation of the TA muscle through the graft and the host nerve. The average peak EMG value (representative of motor unit action potentials) for each stimulus amplitude was calculated for both the graft and host nerves (Figure 3.3). As the frequency of stimulation increased, the strength of muscle contractions increased. The EMG amplitude was

greater in the host nerve as compared to the graft nerve. Specifically, at 80Hz stimulation, the host nerve and graft nerve, the difference between the graft and host nerve amplitudes was 0.53 ± 1.85 mV with the graft being weaker. Additionally, the EMG values were greater in group 2 as compared to group 1 which was interesting to note.

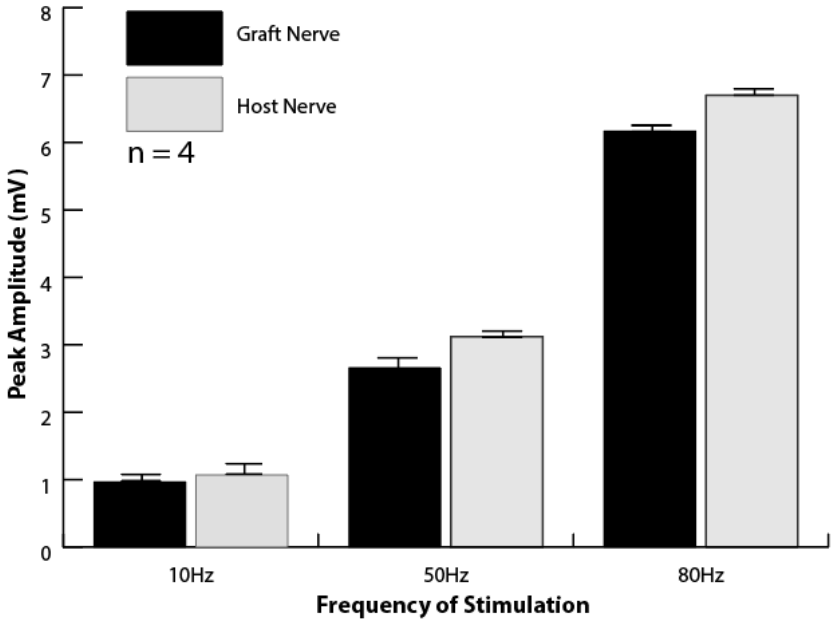

Figure 3.3 Electromyography results. Average peak EMG values for the graft nerve and the host nerve increase in amplitude as stimulation frequency increases. The difference between the peak values for the graft and host nerve at 80Hz is 0.53 ± 1.85 mV.

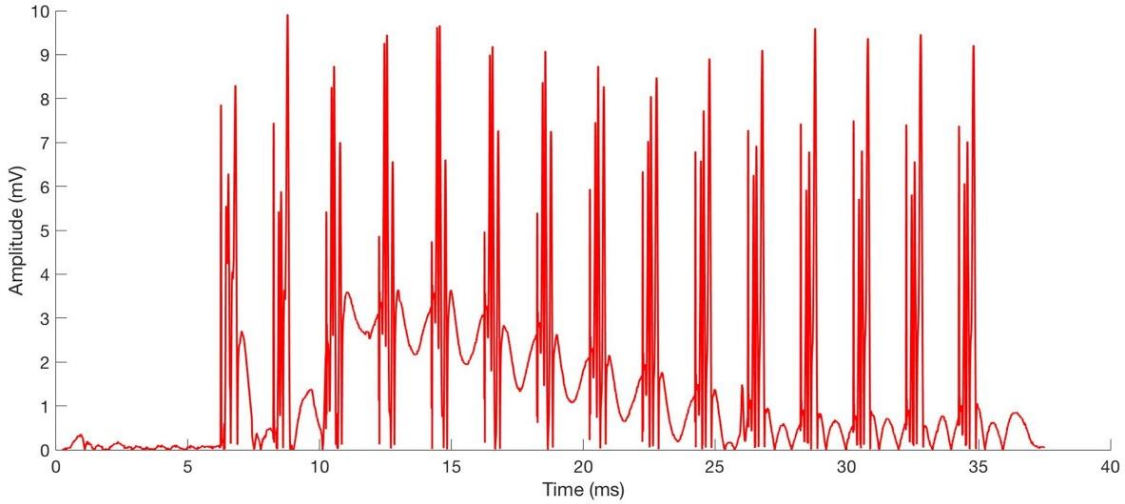

Figure 3.4 Representative electromyograms (EMGs) at 80 Hz recorded distal to the graft nerve transected and regenerated through a silicone conduit. The EMGs were evoked with epineurial hook electrodes at the proximal site of the graft nerve and recorded distally in the TA muscle.

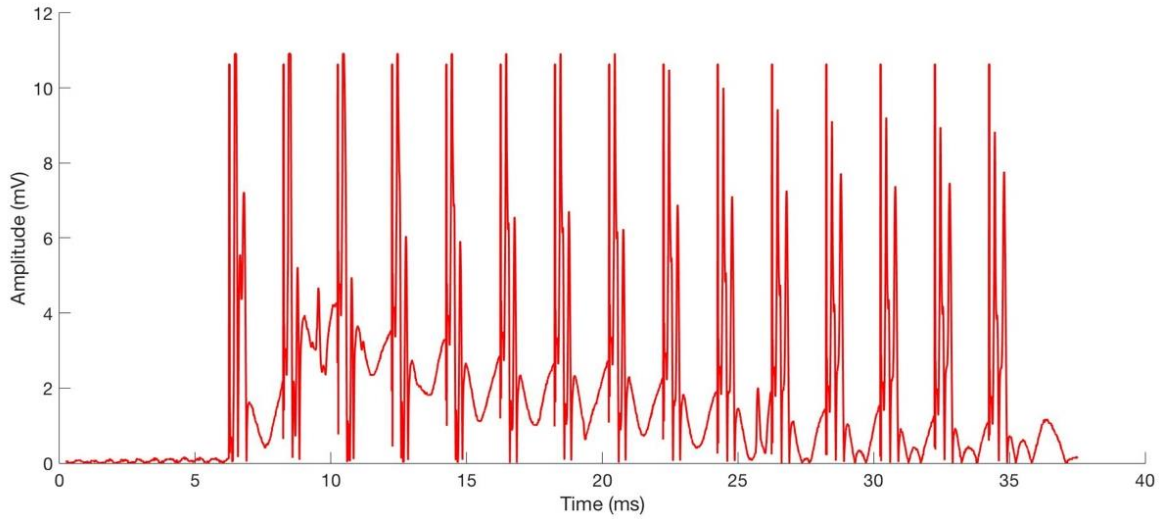

Figure 3.5 Representative electromyograms (EMGs) at 80 Hz recorded distal to the host nerve transected and regenerated through a silicone conduit. The EMGs were evoked with epineurial hook electrodes at the proximal site of the graft nerve and recorded distally in the TA muscle.

3.3.2 Evoked Muscle Force Measurement

Isometric twitch force data indicated an increase in force upon 1 recruitment of motor axons with increasing stimulus amplitude for both the graft and host nerves. Stimulation of both nerves resulted in twitch responses with the greatest active force seen at 1000 μA for both TA and EDL muscles (Figure 3.6; Figure 3.8). The TA and EDL muscle motor axons distal to the graft nerve elicited maximal twitch force measurements similar to the motor axons distal to the host nerve (TA/Graft: 0.85 ± 0.98 N and EDL/Graft: 0.12 ± 0.94 N, TA/Host: 0.92 ± 0.96 N, EDL/Host: 0.12 ± 0.92 N) (Figure 3.7; Figure 3.9). Force production was generally weaker as compared to group 1.

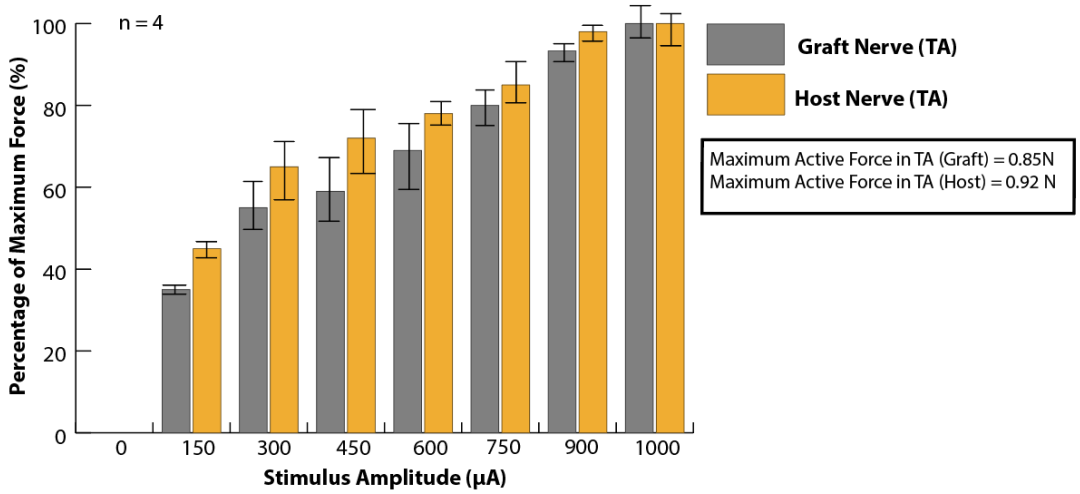

Figure 3.6 Percentage values of twitch force response of TA muscle to stimulation of proximal areas of graft and host nerves. Increased twitch contractions with progressively higher stimulation currents are evident.

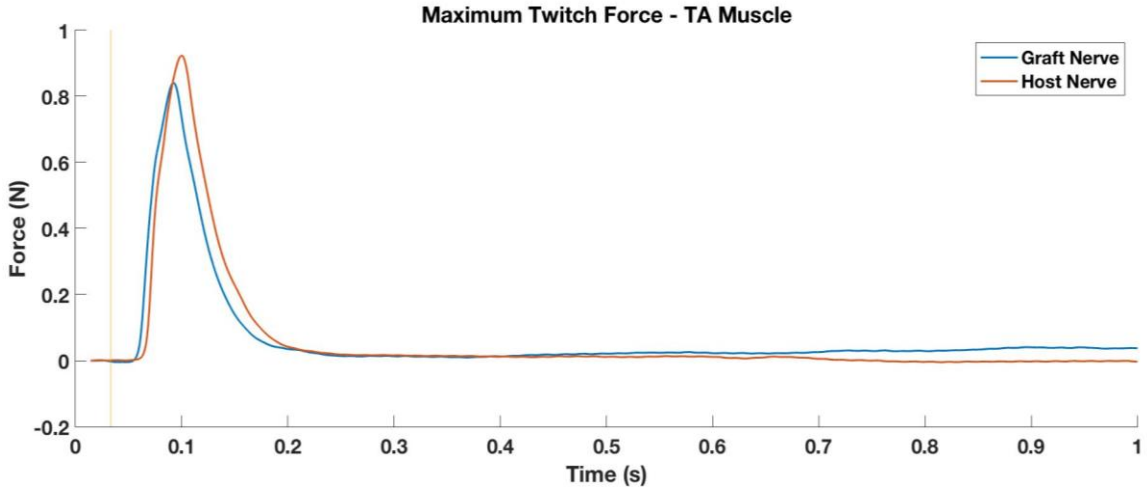

Figure 3.7 TA muscle recruitment curve generated upon stimulation of graft and host nerves at 1000 µA and 0 Hz. Elicited maximal force is greater in the host nerve, explained by the stronger innervation of motor neurons with muscle fibers.

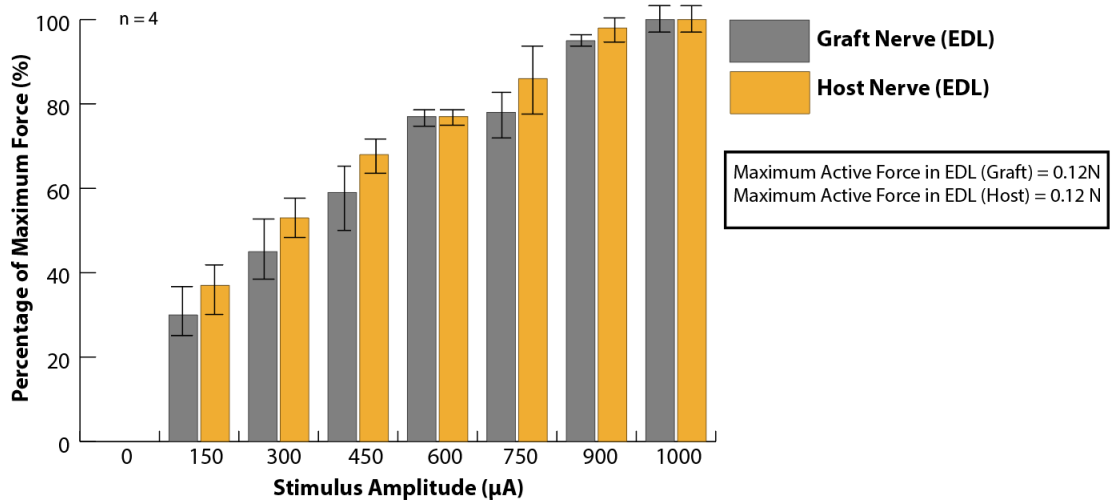

Figure 3.8 Percentage values of twitch force response of EDL muscle to stimulation of proximal areas of graft and host nerves. Increased stimulus results in an increased strength of contraction, seen greatest at 1000 µA. Another point to note is the similar twitch response in the host and graft nerves.

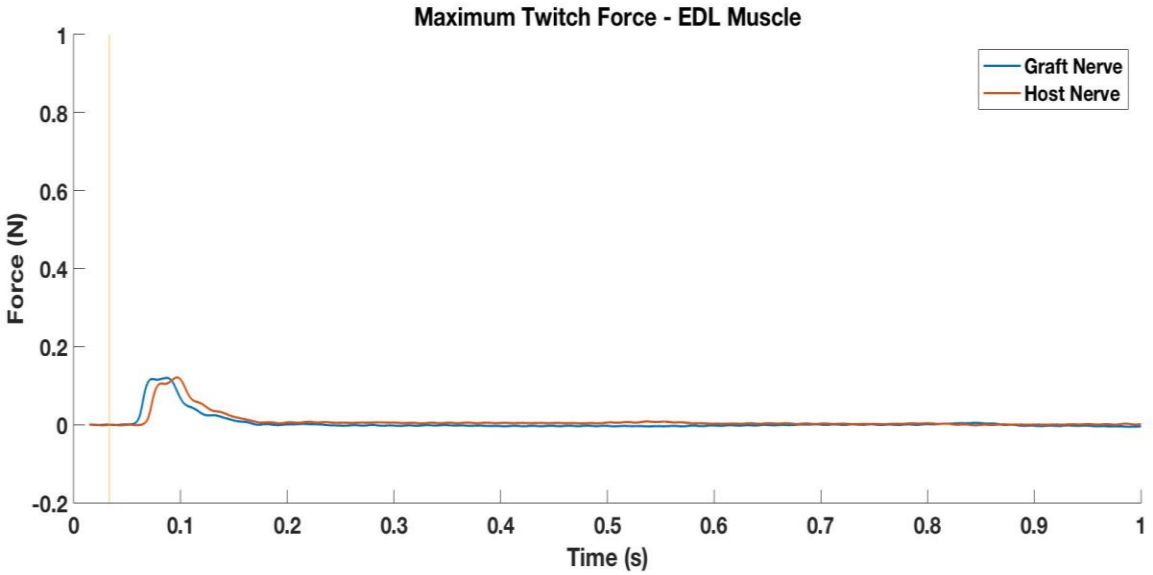

Figure 3.9 EDL muscle recruitment curve generated upon stimulation of the graft and host nerves at 1000 μA and 0 Hz. Elicited maximal force is similar in the host and graft nerves.

Isometric tetanic force data had similar trends with the greatest active force produced at 80 Hz for both the host and graft nerves in both TA and EDL muscles (Figure 3.10; Figure 3.12). The decreasing force values at 100 Hz and 120 Hz can be associated with muscle fatigue as described in chapter 2. The TA and EDL muscle motor axons distal to the graft nerve elicited maximal tetanic force measurements equivalent to the motor axons distal to the host nerve (TA/Graft: 5.42 ± 0.64 N and EDL/Graft: 0.62 ± 0.46 N, TA/Host: 5.50 ± 0.68 N, EDL/Host: 0.56 ± 0.82 N) (Figure 3.11; Figure 3.13). As seen with the twitch force measurements, the TA muscle elicited greater forces as compared to the EDL. Additionally, the host nerve overall elicited a slightly larger force as compared to the graft nerve but were comparable. The tetanic forces were generally weaker than those elicited in group 1.

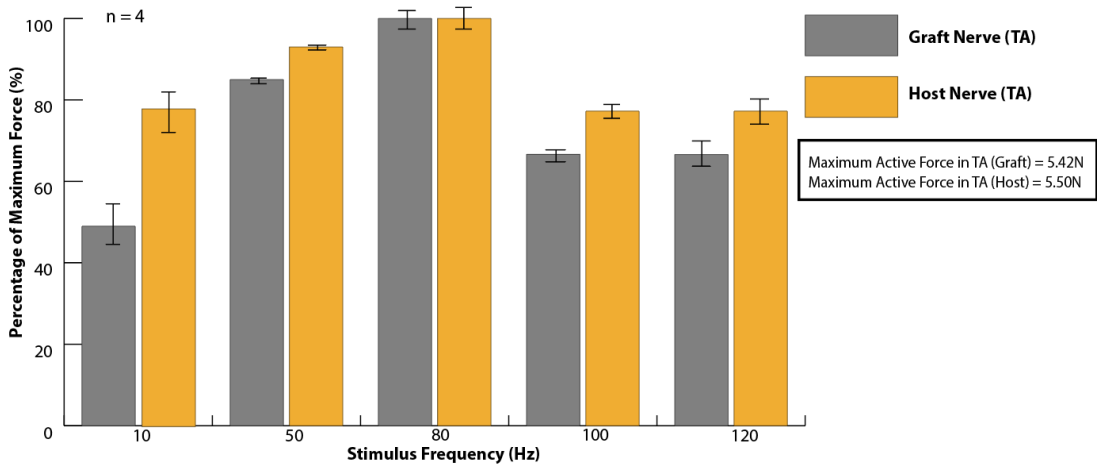

Figure 3.10 Percentage of maximal tetanic force measurements for the TA muscle with the greatest active force at 80 Hz. The decrease in active force at 100 Hz and 120 Hz can we associated with muscle fatigue due to increased strength in muscle contractions as a result of repeated stimulation of action potentials.

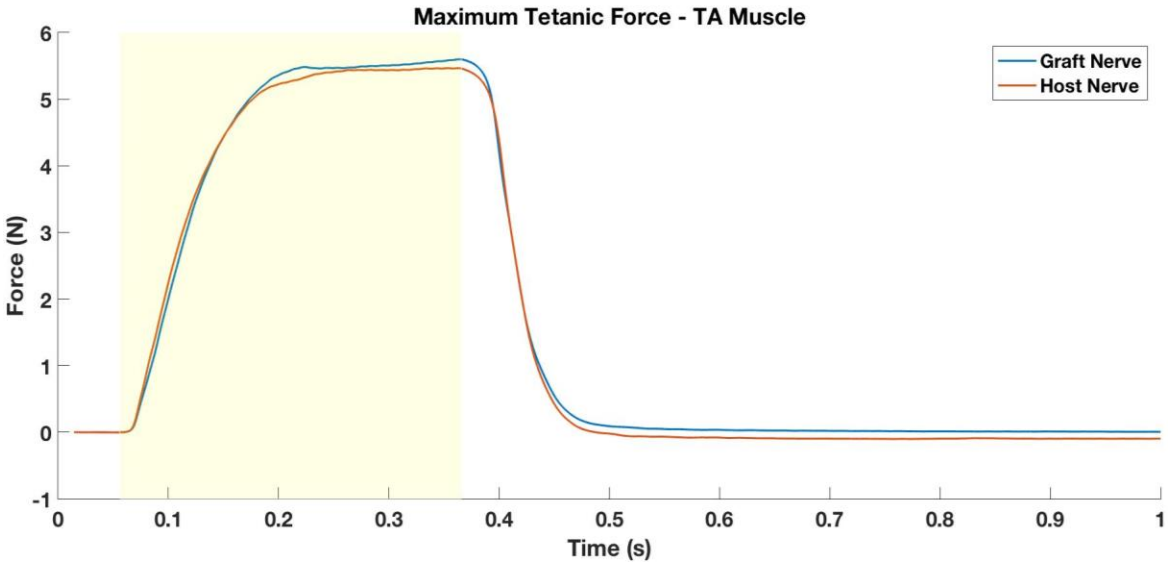

Figure 3.11 Representation TA muscle recruitment at 80 Hz for both host and graft nerves. Maximal tetanic force for both nerves has minor difference of 0.08 ± 0.04 N.

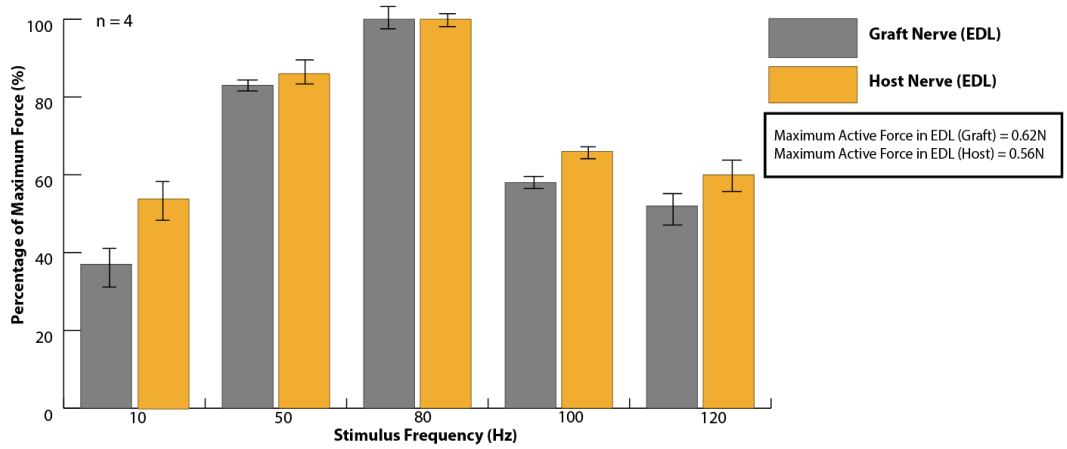

Figure 3.12 Percentage of maximal tetanic force measurements for the EDL muscle with the greatest active force seen at 80 Hz. The decrease in active force at 100 Hz and 120 Hz can we associated with muscle fatigue due to increased strength in muscle contractions as a result of repeated stimulation of action potentials.

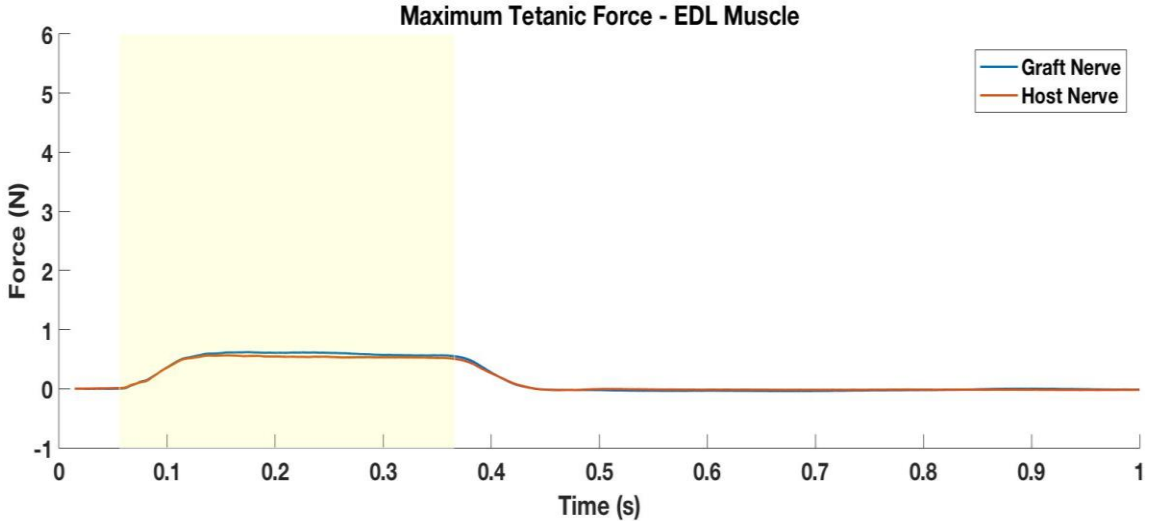

Figure 3.13 Representation of EDL muscle recruitment at 80Hz for both host and graft nerves. Maximal tetanic force for both nerves has minor difference of 0.06 ± 0.36 N with the graft nerve having a greater active force.

Measurement of wet muscle mass demonstrated similar trends to evoked muscle force measurements with the TA muscle having a greater mass. The TA and EDL muscles in this group of animals also had similar masses when compared to the grafted animals and the non-grafted

animals with and without surgery (Figure 3.14). Therefore, performing transecting the nerve and performing the end-to-side surgery did not impact muscle mass.

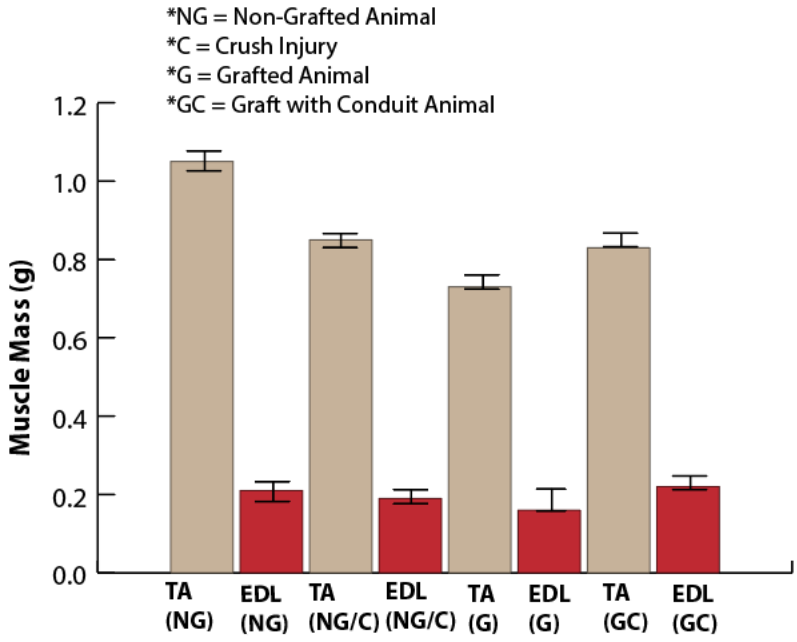

Figure 3.14 Wet muscle mass of TA and EDL muscles following the end-to-side surgery and encapsulation of transected nerve in silicone conduit. The average mass of the TA muscle is slightly lower in the grafted animals while the EDL muscle mass is very similar.

3.4 Conclusions

Placement of the donor nerve in the silicone conduit along with the end-to-side surgery did result in nerve regeneration. 3 months post -surgery, terminal force assessments indicated motor axon innervation of both host and graft nerves with the TA and EDL muscle fibers. The TA and EDL muscles showed similar trends as those discussed in chapter 1. Furthermore, the overall innervation of the graft nerve with musculature was weaker than the host nerve. This is an expected outcome due to the prior innervation of motor axons with distal musculature. Additionally, the active forces produced by the muscles appeared to be overall weaker in this group of animals when compared to the grafted animals. Literature has shown that nerve grafts result in better nerve regeneration and

functionally recovery (Liao, Chen, Wang, & Tseng, 2009) as opposed to nerve conduits. Yet, the EMG values in this group were greater than those measured in group 1. That being said, the evoked force measurements were weaker in group 2 as compared to group 1.

Chapter 4

Group III: End-to-Side Nerve Graft with MSE

The present study examined the utilization of a novel macro-sieve electrode (MSE) in the donor nerve of the end-to-side surgical method. The electrode was designed, fabricated, implanted and evaluated in the *in vivo* rat sciatic nerve model. Electrophysiological evaluation of regenerated nerve fibers looked at motor axon compound action potentials to confirm regeneration of the nerve and innervation with distal musculature.

4.1 Experimental Design

Six adult Lewis rats were utilized in this group. A sciatic nerve was harvested from the left and right limbs of two animals to be used as the graft in the other four animals. In the setup of the surgery, the sciatic nerve harvested from the donor animal was first transected and placed in a silicone conduit which was encased by the macro-sieve electrode. The transected graft nerve was then sutured to the host sciatic nerve at the proximal and distal ends of the exposed nerve (Figure 4.1). The host nerve was injured on the proximal side by means of creating an epineural window to allow for regeneration of axons through the distal portion of the graft.

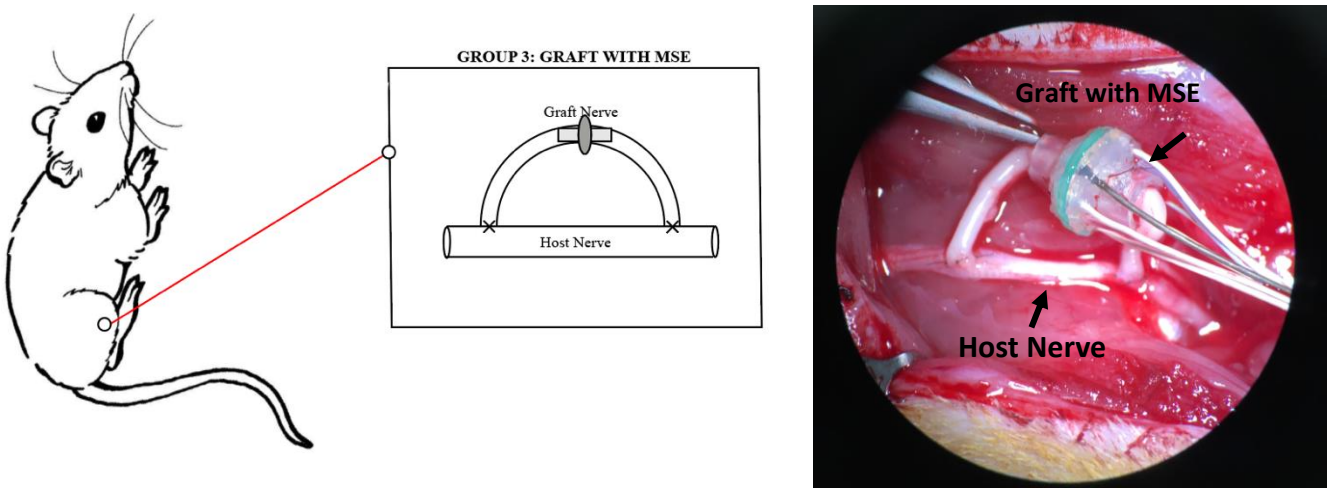

Figure 4.1 Experimental setup. Left panel – a schematic of the surgery. The donor nerve is transected with the proximal side of transection sutured to the left side of the conduit and the distal side sutured to the right side of the conduit. The donor nerve is then sutured to the host sciatic nerve at the sites of the epineural window. Right panel – image of surgery *in vivo*.

4.2 Methods

4.2.1 Fabrication of MSE

Custom sieve electrodes were fabricated out of polyimide (PI-2721, HD Microsystems, Parlin, NJ) gold, and Platinum/Iridium using a method of sacrificial photolithography in the Nano Research Facility at Washington University in St. Louis (St. Louis, MO). Individual sieve electrodes consist of a central porous region, peripheral connector pads, and a micro PCB board. The central porous region (diameter = 2 mm.) comprises nine via-holes each 600 µm. in diameter (transparency = 85%). Eight active electrode sites were positioned between select via-holes throughout the porous area to facilitate neural interfacing. The entire sieve electrode was affixed transversely to the middle of a 10 mm.-long silicone tube (inside diameter = 2 mm.) with biocompatible silicone gel. A razor blade was used to obliquely remove 1 mm from each end of the silicone tube to reduce nerve graft tension. Eight insulated wires emanating from the sieve corresponding to each electrode site were joined to individual channels in an Omnetics connector for data collection. The Omnetics 20-pin connector and approxima of adjacently attached wires were wrapped with moisture-proof sealing film (Parafilm®, Heathrow Scientific, San Diego, CA). The Omnetics 20-pin connector was sterilized with Ethylene Oxide prior to implantation.

4.2.2 Surgical Procedure and Setup

All surgical procedures were conducted with aseptic techniques. The Lewis rats were anesthetized by inhalation using 4% Isoflurane/96% oxygen for induction and 2% Isoflurance/98% oxygen for maintenance administered via nose cone inhalation. For maintenance, the 2% Isoflurane was progressively reduced to 1.5% during the course of the surgery in order to reduce the detrimental effects of prolonged inhalation of Isoflurane. The lateral aspects of lower extremities were shaved and sterilized with 70% isopropyl alcohol followed by 7.5% povidone-iodine solution. Following preparation of the incision site, the sciatic nerve was exposed. 0.9% sodium chloride solution was injected into the conduits before fastening it to adjacent fascia with 5-0 absorbable polyglactin suture (Vicryl™, Ethicon, Somerville, NJ). The emanating wires and Omnetics connector were tunneled subcutaneously to the dorsal cervical region. Micro-scissors were used to create an epineural window on the proximal and distal ends of the exposed nerve. The nerve autografts were micro-surgically implanted in an end-to-side manner and sutured at the points of the epineural windows. At this point, jeweler's forceps were used to administer two subsequent 30-second crush injuries to the native sciatic nerve just distal to the proximal epineurial window to induce axonal sprouting through the window and into the graft. Skin was closed with 4-0 nylon suture (Ethilon™, Ethicon, Somerville, NJ).

4.2.3 Electrophysiological Assessment

Approximately 3 months following implantation, a terminal procedure was performed on each animal. The implanted Onmentics connector was located and an incision was made on its medial side. The scar tissue surrounding the Omentics connector was removed and was rinsed several times with isopropyl alcohol to remove biological fluids that may have entered the connector. The connector was then connected to the TDT MS16 stimulus isolated which was connected to the TDT RX7 base station.

EMG signals were recorded from the TA, EDL, and gastrocnemius (GS) muscles. Positive needle electrodes were placed in each muscle, with negative and ground electrodes placed on the animal's back. These electrodes were connected to a TDT RA16LI-D 16-channel differential head stage

which was connected to a TDT RA16PA 16-channel pre-amplifier. Monopolar stimulations were used, where an anodic needle electrode was added in the animal's tail. The sieve was stimulated using values of 100 μA to 1000 μA. Each stimulus delivered was a biphasic, square, charge-balanced pulse of current 1 ms in length. Each channel was stimulated at every current value in steps of 25 μA.

Following the EMGs, the TA and EDL muscles were explanted and weighed.

4.3 Results

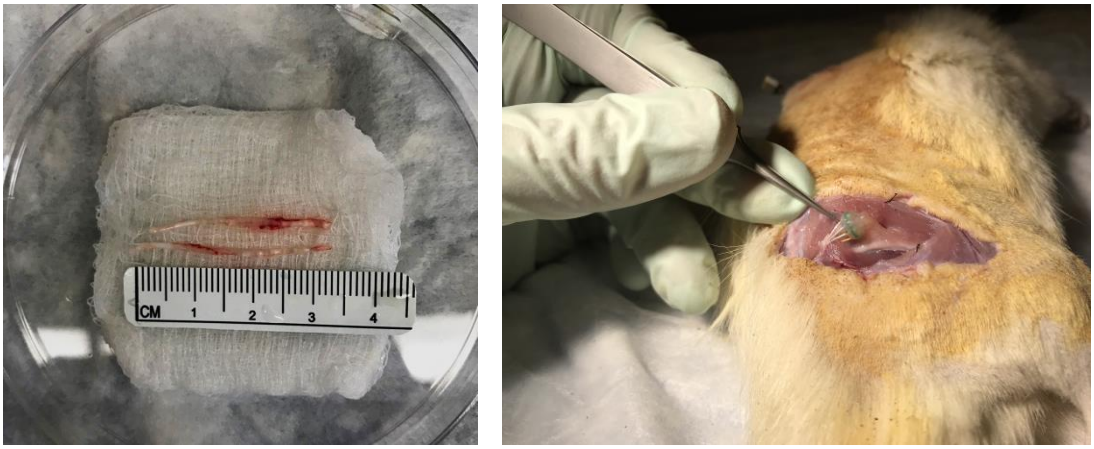

Figure 4.2 Nerve regeneration through sieve electrode. Left – Graft lengths of 32 mm that were implanted in the animal. Right – regeneration of the nerve through the sieve.

4.3.1 Electromyograms

For two of the four animals implanted with the MSE, electrical stimulation of the sciatic nerve at proximal sites of the graft and host nerves evoked EMG responses distally in re-innervated musculature through all 8 channels of the MSE (Figure 4.3; Figure 4.4; Figure 4.5). The EMG recordings showed effective muscle activation of the TA, EDL, and GS muscles through the graft nerve at stimulus amplitudes of 600 μA to 1000 μA for both animals. As expected, the overall amplitudes of the muscles ranked from largest to smallest in the order of TA, EDL, and GS.

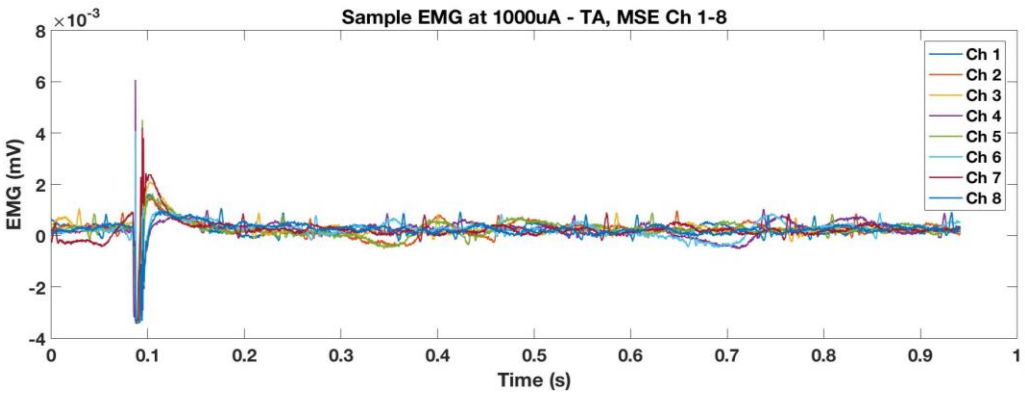

Figure 4.3 Representation of TA muscle EMGs elicited through all 8 channels of the MSE at 1000 μA.

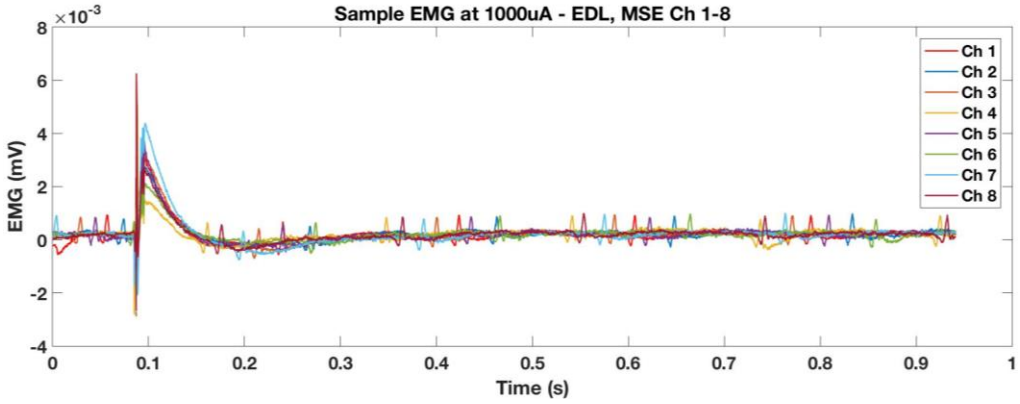

Figure 4.4 Representation of EDL muscle EMGs elicited through all 8 channels of the MSE at 1000 μA.

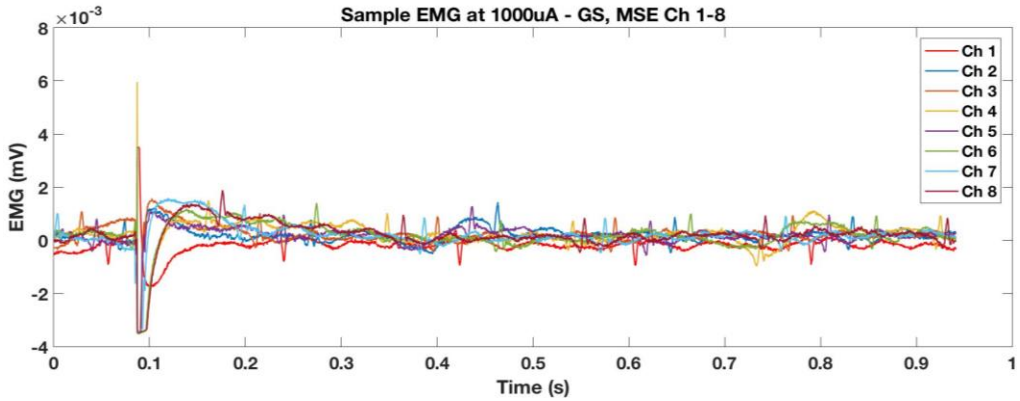

Figure 4.5 Representation of GS muscle EMGs elicited through all 8 channels of the MSE at 1000 μA.

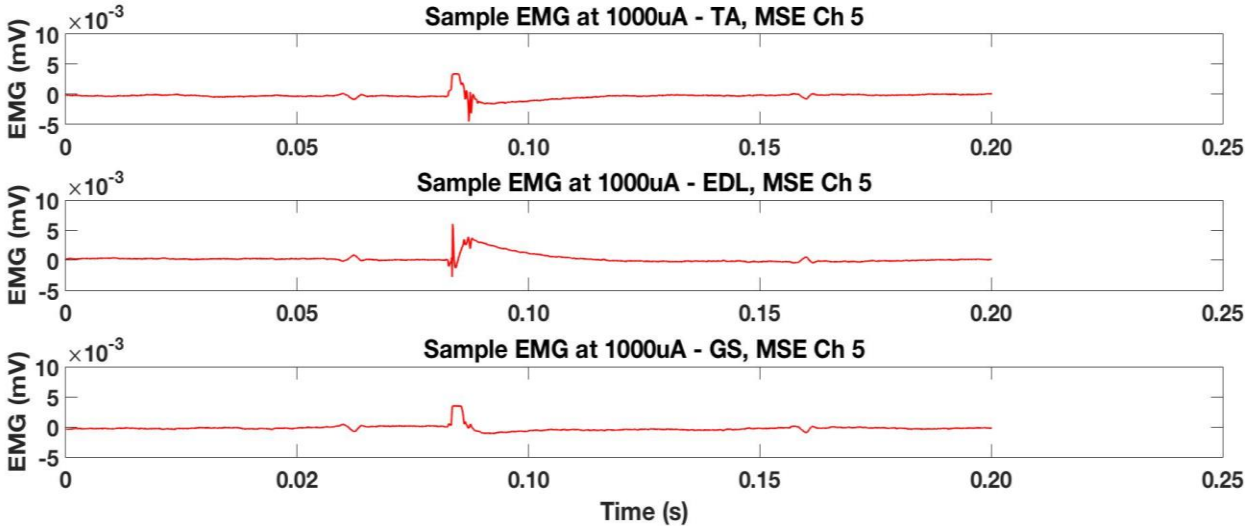

Figure 4.6 Muscle contraction upon stimulation of muscle through channel 5, at 1000 µA. A muscle twitch was evident just after the elicited stimulus indicating innervation of muscle.

4.3.3 Evoked Force Muscle Measurement

Due to muscle dehydration despite constant application of saline, suitable data was not gathered from twitch and tetanic force measurements of the TA, EDL, and GS muscles. TA and EDL wet muscle weighs did indicate that the procedure did not have an impact on the overall muscle mass when compared to the other groups (Figure 4.6).

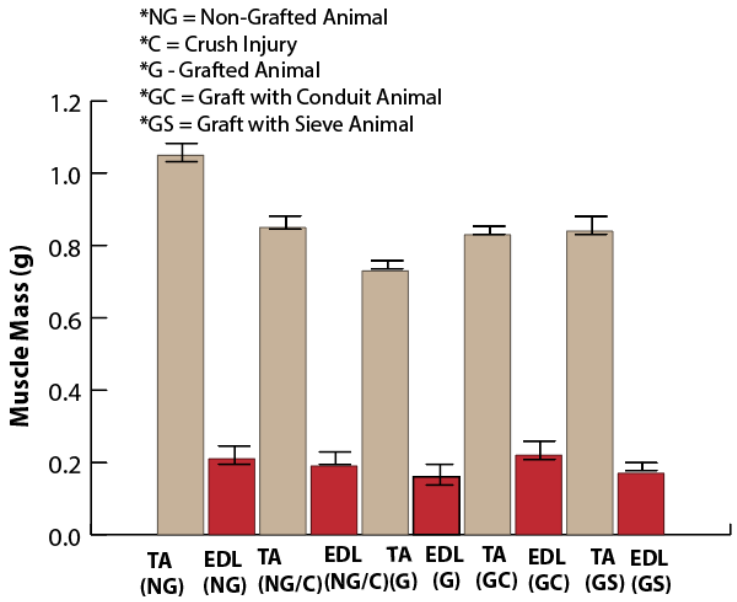

Figure 4.6 Wet muscle mass of TA and EDL muscles following the end-to-side surgery and encapsulation of transected nerve in MSE assembly. The overall weights follow a similar trend as the other groups with the TA being greater than the EDL.

4.4 Conclusions

An overall weakness of this study is that it is unclear whether the regenerated axons are sensory or motor axons. The functional assessments only test for motor axon regeneration. In order to qualitatively identify the axon regeneration, techniques such as retrograde labelling must be done. Fluorophore gold labelling with *in vivo* imaging can allow for visualization of motor endplate reinnervation (Moore et al., 2012).

Furthermore, animals assessed in chapter 2 indicated that the end-to-side nerve graft resulted in robust regeneration and functional recovery. This was consistent with data gathered by other groups that have utilized this surgery technique (Adelson et al., 2004; Liao et al., 2009; Pannucci et al., 2007). Furthermore, the transection of the graft nerve and placement in the silicone conduit also saw robust regeneration in chapter 3. However, the EMG results of group 2 as compared to group 1 were generally greater although the evoked force measurements were weaker. The results of group 2 would be expected to be weaker due to the nerve transection. Literature has shown that regeneration

through conduit elicited EMGs around 6.85 mV while control animals elicited EMG greater than 9 mV (MacEwan et al., 2016). This may have been attributed to the fact that EMG data does not typically provide an accurate quantitative relationship. The hook placement may have been inconsistent while alternating between graft and host nerves repeatedly. Furthermore, saline application could have been insufficient leading to nerve dehydration. Another point of issue could be that the sample size (n = 4) was too small. By increasing the sample size, there would be more consistency with the data.

Current implantation methods of the MSE require transecting the target nerve and placing the thin sieve electrode between proximal and distal nerve stumps (MacEwan et al., 2016). Instead of having to transect a completely healthy and functional nerve, the idea of utilizing a graft nerve with a sieve electrode was assessed. The innervation of the new motor axon network with distal musculature was tested and compared with existing axon networks of the host nerve. All animals with a 3.2 cm graft saw partial or full nerve regeneration through the MSE assembly and innervation of nerve with distal musculature. For two of the animals, stimulation of the MSE did not result in any motor action potentials even at high stimulus amplitudes of 1000 μA although regeneration was visible through the sieve. This showed that there may not have been functional regeneration. The other two animals had innervation of motor axons with muscle fibers. In both cases, twitch responses were visible at stimulus amplitudes of 600 μA and beyond. Although the EMGs showed signs of motor axons regenerating through the interfaces and the conduit and the sieve, evoked force measurements are necessary to quantify the strength of regeneration. It is possible that there may have been inadequate amount of motor axons, or that the high stimulus amplitudes of the EMG resulted in nerve damage or muscle dehydration. Inadequate amount of saline application could have also resulted in muscle dehydration leading to the lack of data. In this case, increasing the sample size would be important for effective assessment of quality in regeneration.

Literature has also shown that the individual electrode sites in MSEs are capable of generating twitch responses at low stimulus amplitudes of 20 – 200 μA as compared to 600 μA as seen in this study (MacEwan et al., 2016). It is possible that the regeneration of axons was non-uniform through the transit zones. In this case, it will be important to assess the histological data to look for equal nerve

bundles through the transit zones. It is also possible that the impedances of the sieve were inconsistent through individual leads. This could have resulted in the electrode being functionally inadequate in targeting the nerve and allowing for optimal recording and stimulation. This does suggest the presence of motor axons but the incapability of the axons to regenerate consistently.

Although evoked isometric force measurements were not gathered from the two animals that did see action potentials, the wet muscle mass indicated that implantation surgery did not affect the overall muscle mass. This also reveals functionality of regenerated nerve fibers crossing the graft nerve and into the distal portions of the host nerve to suggest that there is presence of axonal regeneration and innervation with distal musculature. This present work suggests that it is possible to place the sieve electrode in a transected graft nerve instead of a healthy host nerve when controlling distal musculature and restoring motor function following injury. However, more quantification is required to do so.

4.5 Future Work and Direction

After each terminal functional assessment, the nerves were explanted and fixed in 3% glutaraldehyde in 0.1 M phosphate buffer. The immediate future work will be to compare fiber counts in each group of animals and count nerve bundles through each transit zone of the MSE. This data will show regenerative capabilities and confirm non-uniform regeneration through the MSE. The figures below (Figure 4.7) illustrate the sections that will be taken for each group of animals.

In conducting future experiments, it will be important to assess the impedances of the sieve prior to implantation. Furthermore, increasing sample size to 12 will bring consistency to the data and account for issues such as inconsistent placement of hook electrodes, inadequate application of saline, or the lack evoked force measurements as a result of muscle dehydration. By increasing sample size, functional regeneration through the MSE jump graft can be better quantified.

Another possible solution will be to regenerate nerves through the MSE in donor animals prior to application of donor nerve to target nerves. This will reduce the number of regenerative interfaces to two, similar to the surgery described in chapter 2 but extend the study time to 6 months.

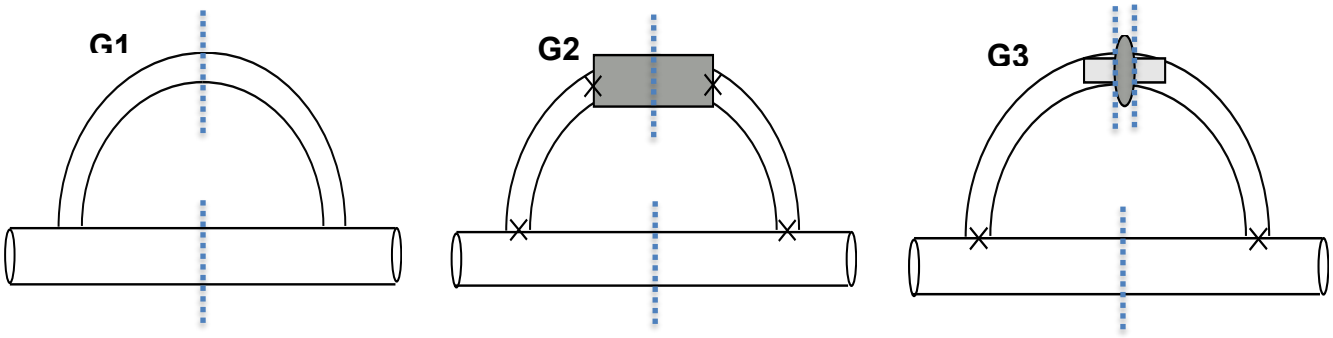

Figure 4.7 Locations of sections for histology for each group. All 1 mm sections will be assessed with fiber counts. Group 1 will be sectioned in the middle of the graft and host nerves respectively, as with group 2. In group 3, it will be important to assess the areas right before and after sieve implantation to assess regeneration.

References

[1] Adelson, P. D., Bonaroti, E. A., Thompson, T. P., Tran, M., & Nystrom, N. A. (2004). End-to-side neurorrhaphies in a rodent model of peripheral nerve injury: a preliminary report of a novel technique. *Journal of Neurosurgery: Pediatrics*, *101*(2), 78–84. https://doi.org/10.3171/ped.2004.101.2.0078

[2] Bradke, F., Fawcett, J. W., & Spira, M. E. (2012). Assembly of a new growth cone after axotomy: the precursor to axon regeneration. *Nature Reviews Neuroscience*, *13*(3), 183–193. https://doi.org/10.1038/nrn3176

[3] Branner, A., Stein, R. B., & Normann, R. A. (2001). Selective Stimulation of Cat Sciatic Nerve Using an Array of Varying-Length Microelectrodes. *Journal of Neurophysiology*, *85*(4), 1585–1594. https://doi.org/10.1152/jn.2001.85.4.1585

[4] Brushart, T. M., Gerber, J., Kessens, P., Chen, Y.-G., & Royall, R. M. (1998). Contributions of Pathway and Neuron to Preferential Motor Reinnervation. *Journal of Neuroscience*, *18*(21), 8674–8681.

[5] Celichowski, J., Krutki, P., Łochyński, D., Grottel, K., & Mróczyński, W. (2004). Tetanic depression in fast motor units of the cat gastrocnemius muscle. *Journal of Physiology and Pharmacology: An Official Journal of the Polish Physiological Society*, *55*(2), 291–303.

[6] Fujiwara, T., Matsuda, K., Kubo, T., Tomita, K., Hattori, R., Masuoka, T., … Hosokawa, K. (2007). Axonal supercharging technique using reverse end-to-side neurorrhaphy in peripheral nerve repair: an experimental study in the rat model. *Journal of Neurosurgery*, *107*(4), 821–829. https://doi.org/10.3171/JNS-07/10/0821

[7] Gurfinkel', V. S., Levik, I. S., & Tsareva, E. B. (1984). [The force of an isometric twitch contraction and the phases of tetanus]. *Biofizika*, *29*(1), 139–142.

[8] Hayashi, A., Pannucci, C., Moradzadeh, A., Kawamura, D., Magill, C., Hunter, D. A., … Myckatyn, T. M. (2008). Axotomy or compression is required for axonal sprouting following end-to-side neurorrhaphy. *Experimental Neurology*, *211*(2), 539–550. https://doi.org/10.1016/j.expneurol.2008.02.031

[9] Higashino, K., Matsuura, T., Suganuma, K., Yukata, K., Nishisho, T., & Yasui, N. (2013). Early changes in muscle atrophy and muscle fiber type conversion after spinal cord transection and peripheral nerve transection in rats. *Journal of Neuroengineering and Rehabilitation*, *10*, 46. https://doi.org/10.1186/1743-0003-10-46

[10] Ijkema-Paassen, J., Meek, M. F., & Gramsbergen, A. (2001). Transection of the sciatic nerve and reinnervation in adult rats: muscle and endplate morphology. *Equine Veterinary Journal*, *33*(S33), 41–45. https://doi.org/10.1111/j.2042-3306.2001.tb05356.x

[11] Koerber, H. R., Seymour, A. W., & Mendell, L. M. (1989). Mismatches between peripheral receptor type and central projections after peripheral nerve regeneration. *Neuroscience Letters*, *99*(1–2), 67–72.

[12] Lago, N., Udina, E., & Navarro, X. (2006). Regenerative electrodes for interfacing injured peripheral nerves: neurobiological assessment. In *The First IEEE/RAS-EMBS International Conference on Biomedical Robotics and Biomechatronics, 2006. BioRob 2006.* (pp. 1149–1153). https://doi.org/10.1109/BIOROB.2006.1639247

[13] Liao, W.-C., Chen, J.-R., Wang, Y.-J., & Tseng, G.-F. (2009). The efficacy of end-to-end and end-to-side nerve repair (neurorrhaphy) in the rat brachial plexus. *Journal of Anatomy*, *215*(5), 506–521. https://doi.org/10.1111/j.1469-7580.2009.01135.x

[14] MacEwan, M. R., Zellmer, E. R., Wheeler, J. J., Burton, H., & Moran, D. W. (2016). Regenerated Sciatic Nerve Axons Stimulated through a Chronically Implanted Macro-Sieve Electrode. *Frontiers in Neuroscience*, *10*. https://doi.org/10.3389/fnins.2016.00557

[15] McDonnall, D., Clark, G. A., & Normann, R. A. (2004). Selective motor unit recruitment via intrafascicular multielectrode stimulation. *Canadian Journal of Physiology and Pharmacology*, *82*(8–9), 599–609. https://doi.org/10.1139/y04-047

[16] Mensinger, A. F., Anderson, D. J., Buchko, C. J., Johnson, M. A., Martin, D. C., Tresco, P. A., … Highstein, S. M. (2000). Chronic recording of regenerating VIIIth nerve axons with a sieve electrode. *Journal of Neurophysiology*, *83*(1), 611–615. https://doi.org/10.1152/jn.2000.83.1.611

[17] Moore, A. M., Borschel, G. H., Santosa, K. A., Flagg, E. R., Tong, A. Y., Kasukurthi, R., … Mackinnon, S. E. (2012). A transgenic rat expressing green fluorescent protein (GFP) in peripheral nerves provides a new hindlimb model for the study of nerve injury and regeneration. *Journal of Neuroscience Methods*, *204*(1), 19–27. https://doi.org/10.1016/j.jneumeth.2011.10.011

[18] Muheremu, A., & Ao, Q. (2015). Past, Present, and Future of Nerve Conduits in the Treatment of Peripheral Nerve Injury [Research article]. https://doi.org/10.1155/2015/237507

[19] Navarro, X., Krueger, T. B., Lago, N., Micera, S., Stieglitz, T., & Dario, P. (2005). A critical review of interfaces with the peripheral nervous system for the control of neuroprostheses and hybrid bionic systems. *Journal of the Peripheral Nervous System: JPNS*, *10*(3), 229–258. https://doi.org/10.1111/j.1085-9489.2005.10303.x

[20] Pabari, A., Lloyd-Hughes, H., Seifalian, A. M., & Mosahebi, A. (2014). Nerve conduits for peripheral nerve surgery. *Plastic and Reconstructive Surgery*, *133*(6), 1420–1430. https://doi.org/10.1097/PRS.0000000000000226

[21] Pannucci, C., Myckatyn, T. M., Mackinnon, S. E., & Hayashi, A. (2007). End-to-side nerve repair: review of the literature. *Restorative Neurology and Neuroscience*, *25*(1), 45–63.

[22] Raez, M. B. I., Hussain, M. S., & Mohd-Yasin, F. (2006). Techniques of EMG signal analysis: detection, processing, classification and applications. *Biological Procedures Online*, *8*, 11. https://doi.org/10.1251/bpo115

[23] Scheib, J., & Höke, A. (2013). Advances in peripheral nerve regeneration. *Nature Reviews Neurology*, *9*(12), 668–676. https://doi.org/10.1038/nrneurol.2013.227

[24] Yoshida, K., & Horch, K. (1993). Selective stimulation of peripheral nerve fibers using dual intrafascicular electrodes. *IEEE Transactions on Biomedical Engineering*, *40*(5), 492–494. https://doi.org/10.1109/10.243412

[25] Yoshimura, K., Asato, H., Cederna, P. S., Urbanchek, M. G., & Kuzon, W. M. (1999). The effect of reinnervation on force production and power output in skeletal muscle. *The Journal of Surgical Research*, *81*(2), 201–208. https://doi.org/10.1006/jsre.1998.5498

Graft-Embedded Regenerative MSEs, Nishtala, M.S. 2018